Since January 2020 Elsevier has created a COVID-19 resource centre with free information in English and Mandarin on the novel coronavirus COVID-19. The COVID-19 resource centre is hosted on Elsevier Connect, the company's public news and information website.

Elsevier hereby grants permission to make all its COVID-19-related research that is available on the COVID-19 resource centre - including this research content - immediately available in PubMed Central and other publicly funded repositories, such as the WHO COVID database with rights for unrestricted research re-use and analyses in any form or by any means with acknowledgement of the original source. These permissions are granted for free by Elsevier for as long as the COVID-19 resource centre remains active.

Journal of Infection 81 (2020) 816–846

Contents lists available at ScienceDirect

Journal of Infection

journal homepage: www.elsevier.com/locate/jinf

Letters to the Editor

Asymptomatic infection and atypical manifestations of COVID-19: Comparison of viral shedding duration

Dear Editor,

Coronavirus disease 2019 (COVID-19) bears several challenging problems, including insidious symptom onset, subclinical manifestations and highly transmissible property during early stage of infection.[1] In the recent study by Huang et al., SARS-CoV-2-infection presented strong infectivity during the incubation period with rapid transmission.[2] Some patients with COVID-19 are asymptomatic, while others complain of atypical symptoms including loss of smell and taste sense.[3] However, there is insufficient data on the prevalence of asymptomatic infection and atypical manifestations of COVID-19. In this study, we aimed to evaluate the prevalence of asymptomatic infection, anosmia (smell loss) and ageusia (taste loss) among patients with mild COVID-19 in a residential treatment center (RTC). We also compared the duration of SARS-CoV-2 viral shedding between groups with different clinical manifestations.

An observational cohort study was conducted for 199 patients with COVID-19 in a RTC at Gyeongju, Gyeongsangbuk province, Republic of Korea (ROK). The RTC was introduced to care patients with mild COVID-19 for the efficient distribution of limited medical resources during large epidemic in early March 2020. Data on demographic findings, symptoms, and duration of viral shedding were collected. The patients were interviewed about initial symptoms and their duration in detail. Real-time PCR (RT-PCR) to detect SARS-CoV-2 was performed every 2–7 days. Duration of viral shedding was considered as time from diagnosis date to the day before first negative conversion of two consecutive negative results of RT-PCR. RT-PCR was conducted using Allplex 2019-nCoV assay (Seegene, Seoul, South Korea). Statistical analyses were performed using SPSS 20.0 program. Mann-Whitney U test was performed to compare the duration of viral shedding between groups with different clinical manifestations. *P*-value < 0.05 was considered statistically significant. This study was approved by the Institutional Review Board of Korea University Guro Hospital (approval number: 2020GR0135).

Among 199 patients with COVID-19, male was 34.7% and mean age of the patients was 38.0 years (Table 1). Most patients (187, 94.0%) were healthy without chronic medical conditions. Among 199 patients, 26.6% were asymptomatic. In the early study, asymptomatic cases accounted for 10.7% (3/28) of COVID-19 cases in the ROK.[1] Asymptomatic proportion of COVID-19 was estimated as 17.9% (95% credible interval, 15.5–20.2%) on the Diamond Princess cruise ship, Japan.[4] Among clinical manifestations, cough (41.2%) was most common, followed by rhinorrhea and nasal stuffiness (30.2%). Of note, 26.1% (52/199) of patients presented anosmia, and 22.6% (45/199) complained of ageusia. Thirty-eight (19.1%) patients complained of both anosmia and ageusia. Duration of anosmia and ageusia ranged 2–28 days (median, 7 days) and 3 - 28 days (median, 7 days), respectively. Recently, substantial number of patients with COVID-19 were reported globally to have developed anosmia or hyposmia.[3,5] Among 59 hospitalized patients with COVID-19, 33.9% reported olfactory or taste disorder in Italy[3]. This is consistent with current observations: among 146 symptomatic patients, 35.6% developed anosmia and 30.8% had ageusia in this study.

Table 1
Demographic and clinical characteristics of the patients with COVID-19 in a residential treatment center ($n = 199$).

Variable	Value
Sex - male, n (%)	69 (34.7)
Age, mean ± SD	38.0 ± 13.1
Chronic medical conditions	12 (6.0)
Diabetes mellitus	5 (2.5)
Hypertension	7 (3.5)
Cerebral infarction	2 (1.0)
Others*	2 (1.0)
Asymptomatic infection	53 (26.6)
Symptoms	
Fever	38 (19.1)
Myalgia	34 (17.1)
Headache	7 (3.5)
Fatigue	8 (4.0)
Cough	82 (41.2)
Sputum	41 (20.6)
Sore throat	15 (7.5)
Rhinorrhea/nasal stuffiness	60 (30.2)
Anosmia	52 (26.1)
Duration, mean ± SD	8.4 ± 6.0
Ageusia	45 (22.6)
Duration, mean ± SD	7.5 ± 5.6
Anorexia	1 (0.5)
Diarrhea	9 (4.5)
Chest pain	7 (3.5)
Pneumonia	5 (2.5)
Duration of viral shedding, mean ± SD	24.5 ± 4.8

SD, standard deviation.
* 1 arthritis, 1 migraine.

Mechanism of anosmia and ageusia induced by SARS-CoV-2 infection was not elucidated. Upper respiratory infection is one of the most common causes of olfactory dysfunction.[6] Coronavirus 229E was detected in nasal discharge of a patient with post-viral olfactory dysfunction.[7] SARS-CoV spread in the brain via the olfactory bulb in human angiotensin-converting enzyme 2 (ACE2) transgenic mice model.[8] SARS-CoV-2 use ACE2 for cell entry and ACE2 is widely expressed in the oral tissues, especially in tongue epithelial cells.[9] Epithelial cells in salivary gland ducts were reported as early target cells of SARS-CoV in macaques model.[10] It may be possible that viral tropism and distribution of ACE2 contribute to the development of anosmia and ageusia in patients with SARS-CoV-2 infection. Further research would be required on the mechanism of post-SARS-CoV-2 infection olfactory and taste dysfunction.

Among the study population, mean duration of viral shedding was 24.5 days. Duration of viral shedding was longer in symp-

https://doi.org/10.1016/j.jinf.2020.05.035
0163-4453/© 2020 The British Infection Association. Published by Elsevier Ltd. All rights reserved.

Table 2
Comparison of the duration of viral shedding according to the clinical manifestations.

	Duration of viral shedding (days, mean ± SD)	*p* value
Asymptomatic	22.6 ± 4.0	< 0.01*
Symptomatic	25.2 ± 4.9	
Fever		
Yes	26.6 ± 5.4	0.08
No	24.7 ± 4.6	
Myalgia		
Yes	26.8 ± 5.4	0.15
No	24.7 ± 4.6	
Headache		
Yes	27.0 ± 4.5	0.15
No	25.1 ± 4.9	
Fatigue		
Yes	21.1 ± 4.7	0.02
No	25.5 ± 4.8	
Cough		
Yes	25.6 ± 5.1	0.18
No	24.7 ± 4.5	
Sputum		
Yes	26.8 ± 4.8	0.03
No	24.6 ± 4.8	
Sore throat		
Yes	27.1 ± 4.2	0.13
No	25.0 ± 4.9	
Rhinorrhea/nasal stuffiness		
Yes	25.9 ± 4.6	0.24
No	24.7 ± 5.0	
Anosmia		
Yes	25.6 ± 4.9	0.48
No	25.0 ± 4.9	
Ageusia		
Yes	25.0 ± 4.7	0.75
No	25.3 ± 5.0	
Diarrhea		
Yes	25.0 ± 6.8	0.98
No	25.2 ± 4.8	
Chest pain		
Yes	30.0 ± 4.7	0.01
No	25.0 ± 4.8	
Pneumonia		
Yes	27.8 ± 3.8	0.20
No	25.1 ± 4.9	

* comparison of asymptomatic cases versus symptomatic cases.

tomatic patients than in asymptomatic patients (25.2 days versus 22.6 days, $p < 0.01$) (Table 2). Particularly among symptomatic patients, those with chest pain released the virus significantly longer (30.0 days versus 25.0 days, $p = 0.01$). Prolonged viral shedding was also found in patients who complained of sputum (26.8 days versus 24.6 days, $p = 0.03$).

This study has some limitations. Anosmia and ageusia were subjective symptoms. Olfactory test was not performed, and quantitative scale of olfactory dysfunction was not measured. In addition, viability of SARS-CoV-2 detected by PCR was not proven using viral culture. However, this study is valuable in that it can provide detailed information about asymptomatic infections and atypical manifestations such as smell or taste dysfunction in patients with COVID-19.

In conclusion, all patients with COVID-19 showed prolonged viral shedding irrespective of clinical manifestations. Asymptomatic patients have potential to spread SARS-CoV-2 without recognition. Thus, mask wearing, hand hygiene and social distancing would be important to control the viral transmission.

Author contributions

JYN and JYS analyzed the data with responsibility for its integrity and prepared the manuscript. All authors contributed to the conception and design of the study and to the interpretation of data. All authors critically revised the manuscript for intellectual content and approved the final draft for submission.

Financial support

This work was supported by a Korea University Guro Hospital grant (O1905231).

Declaration of Competing Interest

The authors declare no conflict of interest.

References

1. Song J.Y., Yun J.G., Noh J.Y., Cheong H.J., Kim W.J. Covid-19 in South Korea - challenges of subclinical manifestations. *N Engl J Med* 2020. doi:10.1056/NEJMc2001801.
2. Huang L., Zhang X., Zhang X., et al. Rapid asymptomatic transmission of COVID-19 during the incubation period demonstrating strong infectivity in a cluster of youngsters aged 16-23 years outside Wuhan and characteristics of young patients with COVID-19: a prospective contact-tracing study. *J Infect* 2020. doi:10.1016/j.jinf.2020.03.006.
3. Giacomelli A., Pezzati L., Conti F., et al. Self-reported olfactory and taste disorders in SARS-CoV-2 patients: a cross-sectional study. *Clin Infect Diseas Offic Publ Infect Diseases Soc Am* 2020. doi:10.1093/cid/ciaa330.
4. Mizumoto K., Kagaya K., Zarebski A., Chowell G. Estimating the asymptomatic proportion of coronavirus disease 2019 (COVID-19) cases on board the Diamond Princess cruise ship, Yokohama, Japan. *Euro Surveill* 2020;**25**(10). doi:10.2807/1560-7917.es.2020.25.10.2000180.
5. Luers J.C., Klussmann J.P., Guntinas-Lichius O. The Covid-19 pandemic and otolaryngology: what it comes down to? *Laryngorhinootologie* 2020. doi:10.1055/a-1095-2344.
6. Deems D.A., Doty R.L., Settle R.G., et al. Smell and taste disorders, a study of 750 patients from the University of pennsylvania smell and taste center. *Arch. Otolaryngol. Head Neck Surg.* 1991;**117**(5):519–28. doi:10.1001/archotol.1991.01870170065015.
7. Suzuki M., Saito K., Min W.P., et al. Identification of viruses in patients with postviral olfactory dysfunction. *Laryngoscope* 2007;**117**(2):272–7. doi:10.1097/01.mlg.0000249922.37381.1e.
8. Netland J., Meyerholz D.K., Moore S., Cassell M., Perlman S. Severe acute respiratory syndrome coronavirus infection causes neuronal death in the absence of encephalitis in mice transgenic for human ACE2. *J. Virol.* 2008;**82**(15):7264–75. doi:10.1128/jvi.00737-08.
9. Xu H., Zhong L., Deng J., et al. High expression of ACE2 receptor of 2019-nCoV on the epithelial cells of oral mucosa. *Int J Oral Sci* 2020;**12**(1):8. doi:10.1038/s41368-020-0074-x.
10. Liu L., Wei Q., Alvarez X., et al. Epithelial cells lining salivary gland ducts are early target cells of severe acute respiratory syndrome coronavirus infection in the upper respiratory tracts of rhesus macaques. *J Virol* 2011;**85**(8):4025–30. doi:10.1128/jvi.02292-10.

Ji Yun Noh
Jin Gu Yoon
Hye Seong
Won Suk Choi
Jang Wook Sohn
Hee Jin Cheong
Woo Joo Kim
Joon Young Song*
Division of Infectious Diseases, Department of Internal Medicine, Korea University College of Medicine, Gurodong-ro 148, Seoul 08308, Republic of Korea
*Corresponding author.
E-mail address: infection@korea.ac.kr (J.Y. Song)

Accepted 17 May 2020
Available online 21 May 2020

https://doi.org/10.1016/j.jinf.2020.05.035

© 2020 The British Infection Association. Published by Elsevier Ltd. All rights reserved.

The potential impact of vulnerability and coping capacity on the pandemic control of COVID-19

Dear Editor,

Worldwide, the coronavirus disease 2019 (COVID-19) has induced a substantial global burden. Since its first diagnosis in Wuhan, China, its spread has affected 216 countries.[1] As of 16 May, 2020, there were more than 4.4 million cases and greater than 302,000 confirmed deaths among patients with COVID-19. Arguably, some nations with lower capacity to cope with the pandemic, especially in low and middle-income countries, might have poorer control of the disease. However, no previous study has proven this association. On the contrary, a recent study published in *the Journal of Infection* examined the association between country-specific global health security index (GHSI) and the burden of COVID-19, but the findings showed that countries with higher GHSI did not have higher COVID-19 rate and had greater number of COVID-19 cases and deaths.[2] Hence, further exploration of the association between country capacity and COVID-19 burden is needed based on other indicators.

The Joint Research Centre (JRC) of European commission has developed an index for risk management named "INFORM",[3] which is a composite indicator based on risk concepts published in the literature. The INFORM model identifies countries at risk of disasters and crisis that could overwhelm response capacity for each country. It ranks countries based on their likelihood of requiring global assistance; synthesizes a risk profile for each country that demonstrates the degree of individual components at risk; and enables trend analysis.[3] Two of its dimensions, namely vulnerability and lack of coping capacity, are particularly relevant to the COVID-19 pandemic. Vulnerability refers to the susceptibility of populations to hazardous incidents, and the lack of coping capacity represents inadequacy of resources that can alleviate the impact of pandemics. The vulnerability dimension could be further subdivided into socioeconomic factors (development and deprivation [50%], inequality [25%], and aid dependency [25%]) and vulnerable groups (uprooted people or other groups). It represents the economic, political and social features of the populations that can be destabilised in the event of a hazardous incident.[3] The lack of coping capacity measures if a country is unable to cope with disasters through the government's effort and existing infrastructure. It could be institutional (disaster risk reduction and governance) or infrastructure-related (communication, physical infrastructure, and access to health systems). We aimed to evaluate if countries with lower vulnerability and higher coping capacity were associated with better control of the COVID-19 pandemic, as measured by incidence and mortality outcomes.

We established a panel of experts consisting of epidemiologists, physicians, and public health professionals who were tasked to determine the outcomes used in this study based on literature review. After discussion the panel determined the following outcome variables: the maximum 14-day cumulative incidence rate per 100,000 population since the first case (22 January to 30 April, 2020); and the incidence and mortality per 100,000 population within 30 days since the first COVID-19 diagnosis and first COVID-19 related death, respectively, from the Johns Hopkins Centre for Systems Science and Engineering (CSSE).[4] The variables tested for association with these outcomes included the COVID-19 vulnerability and the COVID-19 lack of coping capacity as of 2018. Three linear regression models were constructed for the three outcomes whilst adjusting for Gross Domestic Product (GDP) of the same year for each nation;[5] and the population density of each country from the World Population Review.[6] The study was approved by the Survey and Behavioral Research Ethics Committee of the Chinese University of Hong Kong (SBRE-19-592). All p values $\leq$ 0.05 were considered statistically significant.

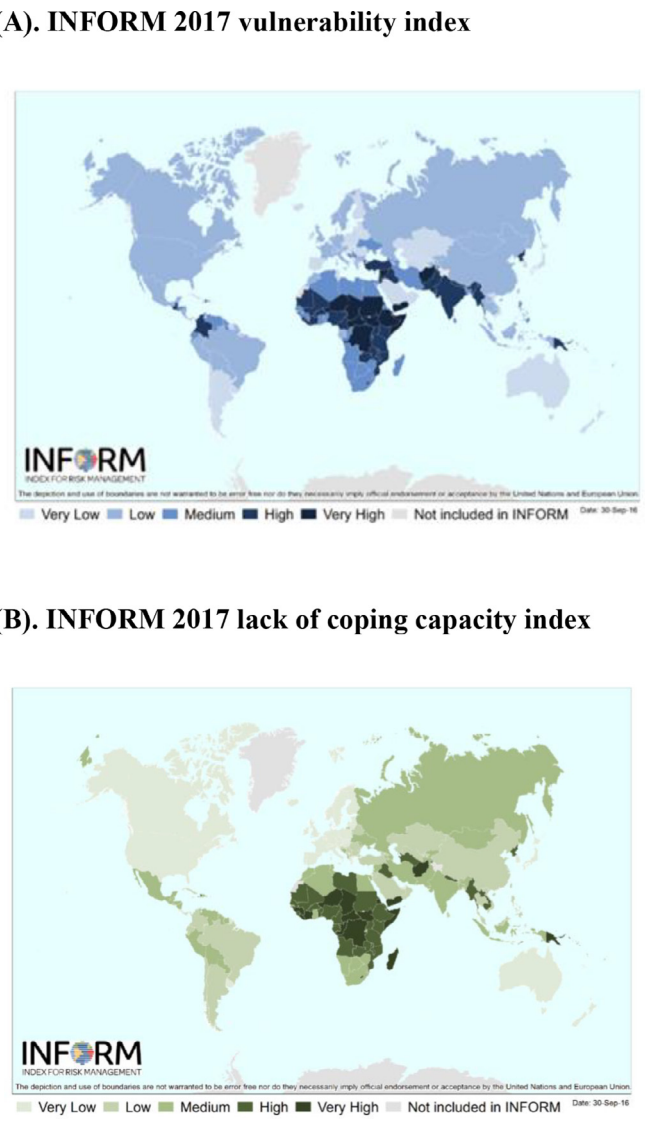

Fig. 1. The distribution of COVID-19 vulnerability index and COVID-19 lack of coping capacity index
Source: Source of Figures: Marin-Ferrer M, Vernaccini L, Poljansek, K. Index for Risk Management INFORM Concept and Methodology Report – Version 2017, EUR 28655 EN, doi:10.2760/094023 https://publications.jrc.ec.europa.eu/repository/bitstream/JRC106949/kjna28655enn.pdf

The distribution of vulnerability and coping capacity scores was shown in Fig. 1. The COVID-19 vulnerability score was the highest in Italy (score 8.2 out of 10), Japan (8.2), Croatia (8.1) and Latvia (8.1). Countries with the severest lack of coping capacity included Central African Republic (9.4), Comoros (9.1), Equatorial Guinea (7.7), and Burundi (7.6). From multivariate regression analysis (Table 1), countries with higher vulnerability were significantly associated with higher maximum 14-day cumulative incidence since the first case (β coefficient 7.54, 95% C.I. 2.82, 12.27, p=0.002), as well as the incidence (β coefficient 3.52, 95% C.I. 0.94, 6.11, p=0.008) and mortality (β coefficient 0.50, 95% C.I. 0.17, 0.84, p=0.003) per 100,000 population within 30 days since the first COVID-19 diagnosis and first COVID-19 related death, respectively. On the contrary, higher coping capacity was associated with lower maximum 14-day cumulative incidence (β coefficient -8.54, 95% C.I. -12.41, -4.68, p<0.001), and lower incidence (β coefficient

Table 1
The association between vulnerability index, ability to cope score and the incidence/mortality outcomes related to COVID.

	Incidence outcome (A)				Incidence outcome (B)				Mortality outcome (C)			
	β coefficients	95% CI		p	β coefficients	95% CI		p	β coefficients	95% CI		p
COVID-19 Vulnerability index	7.54	2.82	12.27	0.002	3.52	0.94	6.11	0.008	0.50	0.17	0.84	0.003
COVID-19 Coping capacity	-8.54	-12.41	-4.68	<0.001	-3.09	-5.00	-1.18	0.002	-0.34	-0.64	-0.04	0.028

The linear regression models were controlled for Gross Domestic Product (GDP) and population density. Incidence outcome (A): the maximum 14-day cumulative incidence rate per 100,000 population since the first case from 22 January to 30 April, 2020; Incidence outcome (B): the incidence per 100,000 population within 30 days since the first COVID-19 diagnosis; and Mortality outcome: (C). the mortality per 100,000 population within 30 days since the first COVID-19 related death.

-3.09, 95% C.I. -5.00, -1.18, p=0.002) and mortality (β coefficient -0.34, 95% C.I. -0.64, -0.04, p=0.028) per 100,000 population within 30 days. There was no interaction or multicollinearity among the covariates.

Our findings imply that reducing vulnerability and enhancing capacity to cope could potentially mitigate the COVID-19 pandemic. Since the components of the two predictor variables are modifiable, countries that aim to increase their capability to combat the COVID-19 pandemics could make reference to the detailed subcategories under these two dimensions. The government could consider to take active steps in enhancing the resilience of the society and availability of measures that could protect the vulnerable population. Nevertheless, there are limitations of our study. Firstly, there may be other confounders that could not be controlled for, including personal behaviour and the stringency of Governmental policies,[7] such as measures related to social distancing, school closure, supply of personal protective equipment (PPE), as well as quarantine and containment strategies.[8-10] In addition, the COVID-19 vulnerability used was developed in 2018, and we assumed that the index of each country did not change before the beginning of the pandemic in 2019. Also, we should emphasize that these are preliminary findings, and the cause-and-effect relationships are yet to be further examined by larger-scale studies.

In conclusion, we identified vulnerability and ability to cope as two important aspects in the face of an infectious disease pandemic, and they bear a potential impact to mitigate the COVID-19 pandemic. Future studies should evaluate the specific components of these indices that exert the greatest impact on pandemic control.

Declaration of Competing Interest

None declared

Acknowledgment

We are grateful for the technical assistance offered by Mr. Peter Choi of the School of Public Health and Primary Care, The Chinese University of Hong Kong

Funding

None

References

1. WHO. Coronavirus disease (COVID-19) outbreak situation. Available at: https://www.who.int/emergencies/diseases/novel-coronavirus-2019. Accessed on 10 May, 2020.
2. Aitken T, Chin KL, Liew D, Ofori-Asenso R. Rethinking pandemic preparation: Global Health Security Index (GHSI) is predictive of COVID-19 burden, but in the opposite direction. *J Infect* 2020 May 8 S0163-4453(20)30273-5Online ahead of print. doi:10.1016/j.jinf.2020.05.001.
3. Marin-Ferrer M, Vernaccini L, Poljansek, K. Index for Risk Management INFORM Concept and Methodology Report — Version 2017, EUR 28655 EN, doi:10.2760/094023
4. The 2019 Novel Coronavirus COVID-19 (2019-nCoV) data repository by Johns Hopkins Centre for Systems Science and Engineering (CSSE). Available at: https://systems.jhu.edu/research/public-health/ncov/. Accessed on 10 May, 2020.
5. The Economist Intelligence Unit, World Bank and Central Intelligence Agency World Factbook. Available at: https://www.cia.gov/library/publications/the-world-factbook/geos/we.html. Accessed on 10 May, 2020.
6. Countries by density by population 2020. World Population Review. Available at: https://worldpopulationreview.com/countries/countries-by-density/. Accessed on 27 April, 2020.
7. University of Oxford. Variation in Government responses to COVID-19. Available at: https://www.bsg.ox.ac.uk/research/publications/variation-government-responses-covid-19. Accessed on 08 May, 2020.
8. Prem K, Liu Y, Russell TW, Kucharski AJ, Eggo RM, Davies N. et al. The effect of control strategies to reduce social mixing on outcomes of the COVID-19 epidemic in Wuhan, China: a modelling study. *Lancet Public Health* 2020;**5**:e261–70.
9. Pan A, Liu L, Wang C, Guo H, Hao X, Wang Q, et al. Association of Public Health Interventions With the Epidemiology of the COVID-19 Outbreak in Wuhan, China. *JAMA* 2020 Apr 10. doi:10.1001/jama.2020.6130.
10. Anderson RM, Heesterbeek H, Klinkenberg D, Hollingsworth TD.. How will country-based mitigation measures influence the course of the COVID-19 epidemic? *Lancet* 2020;**395**:931–4.

Martin CS Wong, MBChB, MD, MPH, FRCP (Edin)*
JC School of Public Health and Primary Care; Faculty of Medicine, The Chinese University of Hong Kong

Jeremy YC Teoh, MBBS, FRCSEd, FCSHK
Office of Global Engagement; Faculty of Medicine, The Chinese University of Hong Kong
Department of Surgery; Faculty of Medicine, The Chinese University of Hong Kong

Junjie Huang, MD, MSc
JC School of Public Health and Primary Care; Faculty of Medicine, The Chinese University of Hong Kong

Sunny H Wong, MBChB (Hons), DPhil (Oxon), FRCP (Edin), FRCPath
Department of Medicine and Therapeutics; Faculty of Medicine, The Chinese University of Hong Kong.

*Correspondence: Martin CS Wong MBChB, MD, MPH, FRCP (Edin), Professor, JC School of Public Health and Primary Care, Faculty of Medicine, The Chinese University of Hong Kong. Tel: (852) 2252 8782; Fax: (852) 2606 3500; Address: 4/F, School of Public Health, Prince of Wales Hospital, Shatin, N.T., Hong Kong
E-mail address: wong_martin@cuhk.edu.hk (M.C. Wong)

Accepted 25 May 2020
Available online 28 May 2020

https://doi.org/10.1016/j.jinf.2020.05.060

© 2020 The British Infection Association. Published by Elsevier Ltd. All rights reserved.

An Early Warning Score to predict ICU admission in COVID-19 positive patients

Dear Editor,

The severe acute respiratory syndrome coronavirus 2 (SARS-CoV-2) that causes coronavirus disease 2019 (COVID-19) poses multiple challenges to our healthcare systems. A particular challenge is the surge of hospital admissions with a significant fraction requiring transfer to intensive care units (ICU) because of respiratory failure.[1,2] Early recognition of patients requiring ICU admission is a critical step in the management of COVID-19 patients. We read with interest the communication in this Journal from Su and colleagues who investigated the utility of clinical scoring systems to predict ICU requirement in patients with COVID-19.[3] Scoring at admission may however be fraught with heterogeneity due to the timing of presentation. Here, we asked whether a monitoring tool on the wards could help identify patients that would require intensive care up to 36 hours in advance. Early warning scores have been developed as composite scores to quantify patient's deterioration.[4] We reviewed data from 36 consecutive PCR-positive COVID-19 patients admitted to the medical wards of the Lausanne University Hospital between March 2, 2020 and March 17, 2020 and examined whether a modified version of the Early Warning Score (EWS) described by Prytherch et al.[4] could contribute to an early identification of COVID-19 patients requiring ICU admission. All variables described by Prytherch et al. were included except for the AVPU variable, which is only documented in a subset of departments at our hospital. Physiological variables were analyzed during a 12 to 36-hour period prior to ICU admission (ICU group) or prior to the most abnormal respiratory variables (i.e. FiO2 or respiratory rate) (non-ICU group) defined as t_0. EWS was calculated at 12-hour intervals prior t_0. Among the 36 patients, 9 were excluded for the following reasons: incomplete or single set of physiological variables (7 patients), pregnancy or immediate ICU admission (1 patient each). Nine required ICU admission and 17 did not. The median age (range) of patients was 74 yr (39-86) in the ICU group and 65.5 yr (26-83) in the non-ICU group (p=0.793). Mean duration of symptoms prior to t_0 was 7.8 days in the ICU-group and 7.6 days in the non-ICU group. Risk factors[2] associated with severe COVID-19 were present in 80.8% of the patients (ICU group: 77.7% and non-ICU group: 82.3%). Fig. 1 shows the evolution of the EWS over a study period up to 36 hours prior t_0 in the two groups of patients. The median EWS was significantly higher in a time-dependent manner in ICU group than in the non-ICU group (p<0.0001) as assessed by mixed effects model[5]. At t_0 or t_{-12} hours, an EWS greater than 7 predicted ICU admission with sensitivities and specificities of 87% and 93% and 94% and 78%, respectively (AUROC 0.98 and 0.88, respectively).

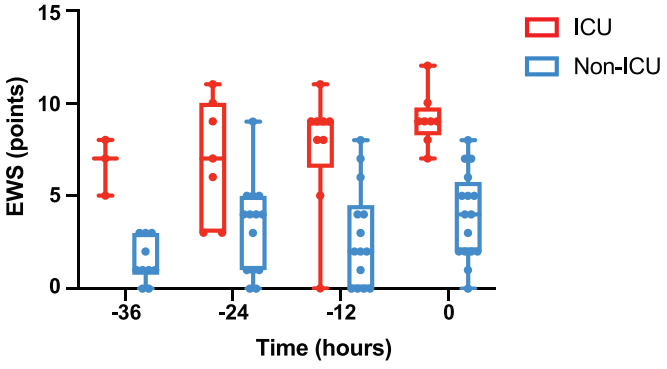

Fig. 1. Evolution of the Early Warning Score (EWS) over time in the two groups of patients. EWS was assessed at 12-h intervals over a 36-hour time period. Time zero refers to the time at which the last set of physiological variables was recorded prior to ICU admission (ICU group, red) or to the worst respiratory variables (non-ICU group, blue). Median (range) EWS was 1 (0-3) vs 7 (5-8) (p= 0.25) at -36-h; 4 (0-9) vs 7 (3-11) (p = 0.1875) at -24-h, 2 (0-8) vs 9 (0-11) (p = 0.0078) at –12-h and 9 (7-12) vs 4 (0-8) (p= 0.0078) at -0h (Wilcoxon test). Number of patients per treatment group at each time point (-36h: 3 vs. 11; -24h: 7 vs 12, -12h: 9 vs 15, 0h: 8 vs 17).

These data suggest that EWS may help clinicians identify in advance COVID-19 patients who will require ICU admission. The low number of patients considered and its retrospective and single-center setting limits this study. Still, in time of patient surge, this simple tool may prove useful for initial triage in the emergency department and subsequent monitoring of patients upon admission to hospital wards.

Declarations

- The CER-VD (ref. nbr. 2020-00776) waived consent to participate and consent for publication for this research according to ORH art. 34 (Switzerland).
- No funding was required for this work.
- Authors' contribution: Study design: SM; Literature search SM, RA; Data collection: SM, PAB, JR, FD, Figure SM, TC, Writing SM, TC, RA.
- Author Information: SM, JR, TC: Infectious Diseases Service, Department of Medicine, Lausanne University Hospital and University of Lausanne, Lausanne, Switzerland. RA Service of Geriatric Medicine and Geriatric Rehabilitation, Lausanne University Hospital, Lausanne, Switzerland. PAB Department of Medicine, Internal Medicine, Lausanne University Hospital, Lausanne, Switzerland. FD Emergency department, Lausanne University Hospital, Switzerland.

Acknowledgements

We wish to thank Raphael Burger of the Internal Medicine Department of Lausanne University Hospital, Isabelle Guilleret, Vassili Soumas and Fady Fares at the Clinical Trial Unit of Lausanne University Hospital as well as Patrick Francioli.

References

1. Grasselli G., Pesenti A., Cecconi M.. Critical Care Utilization for the COVID-19 Outbreak in Lombardy. *Jama* 2020;**323**. doi:10.1001/jama.2020.4031.
2. Guan W., Ni Z., Hu Y., et al. Clinical Characteristics of Coronavirus Disease 2019 in China. *New Engl J Med* 2020. doi:10.1056/nejmoa2002032.
3. Su Y., Tu G.-W., Ju M.-J., et al. Comparison of CRB-65 and quick sepsis-related organ failure assessment for predicting the need for intensive respiratory or vasopressor support in patients with COVID-19. *J Infect* 2020. doi:10.1016/j.jinf.2020.05.007.
4. Prytherch D.R., Smith G.B., Schmidt P.E., Featherstone P.I.. ViEWS—Towards a national early warning score for detecting adult inpatient deterioration. *Resuscitation* 2010;**81**:932–7.
5. McLean R.A., Sanders W.L., Stroup W.W.. A Unified Approach to Mixed Linear Models. *Am Statistician* 1991;**45**:54.

Sylvain Meylan*
Infectious Diseases Service, Department of Medicine, Lausanne University Hospital and University of Lausanne, Lausanne, Switzerland

Rachid Akrour
Service of Geriatric Medicine and Geriatric Rehabilitation, Lausanne University Hospital, Lausanne, Switzerland

Jean Regina
Infectious Diseases Service, Department of Medicine, Lausanne University Hospital and University of Lausanne, Lausanne, Switzerland

Pierre-Alexandre Bart
Department of Medicine, Internal Medicine, Lausanne University Hospital, Lausanne, Switzerland

Fabrice Dami
Emergency department, Lausanne University Hospital, Switzerland

Thierry Calandra
Infectious Diseases Service, Department of Medicine, Lausanne University Hospital and University of Lausanne, Lausanne, Switzerland

*Corresponding author
E-mail address: sylvain.meylan@chuv.ch (S. Meylan)

Accepted 23 May 2020
Available online 28 May 2020

https://doi.org/10.1016/j.jinf.2020.05.047

© 2020 The British Infection Association. Published by Elsevier Ltd. All rights reserved.

Clinical recurrences of COVID-19 symptoms after recovery: Viral relapse, reinfection or inflammatory rebound?

Dear Editor,

The rapidly spreading COVID-19 pandemic resulted in more than 8.5 million cases diagnosed and 450,000 deaths on June 20th, 2020. As described with other coronaviruses, SARS-CoV-2 was first expected to induce a monophasic disease with at least transient immunity.[1,2] Nevertheless, rare cases of suspected COVID-19 "recurrence" or "reactivation" have been reported, including the description by Ye & Colleagues in this journal of 5 patients with suspected SARS-CoV-2 reactivation after home discharge.[3–6]

Similarly, the COCOREC (Collaborative study COvid RECurrences) study aimed at summarizing clinical and virological data of patients presenting a second confirmed COVID-19 episode, at least 21 days after the first onset, and after a symptom-free interval [oxygen-free and discharge from acute-care unit (ACU), or return to usual clinical state]. Cases were collected retrospectively at a multicenter observational level through the COCLICO (COllaborative CLInician COVID-19) French study group meeting. A COVID-19 episode was defined by (*i*) at least one recent major clinical sign of COVID-19 including fever or chills, febrile flu-like-syndrome, dyspnoea, anosmia, or dysgeusia; and (*ii*) a positive SARS-CoV-2 RT-PCR test. Patients were not included if a differential diagnosis (amongst which bacterial, fungal or other viral superinfection, thrombo-embolic complication, secondary organizing pneumonia or interstitial lung disease) could explain the symptom recurrence. After information, all patients agreed with the use of their anonymous medical data. The study has been approved by the Ethic Committee of French Speaking Society of Infectious Disease (CERMIT), number 2020-0503 COVID.

Between April 6th and May 14th, 2020, 11 patients were identified (sex ratio M/F 1.2, median age 55, range [19–91] years). The median duration of symptoms was 18 [13–41] days for the first episode and 10 [7–29] days for the second one for the 7 patients who eventually recovered. Epidemiological and clinical data are summarized in Table 1.

Four healthcare workers (patients 1–4, median age 32.5 [19–43] years) without significant comorbidity had a first mild COVID-19 episode with a complete recovery: three returned to work in COVID units, one had possible COVID re-exposure at home (patient 2). All of them experienced a clinical relapse requiring sick-leave but no hospitalization after a median symptom-free interval of 9 [7–14] days.

In contrast, 7 older comorbid patients (patients 5–11, median age 73 [54–91] years) required ACU hospitalization for both episodes, with a clinical recovery of 11 [4–27] days in the interval. During the first episode, one patient received lopinavir, and three corticosteroids. Six of them required oxygen therapy again during the second episode. Two patients died of ARDS recurrence and another of chronic right heart failure worsening.

All patients had a positive SARS-CoV-2 RT-PCR test in respiratory samples for both episodes (Table 2). They all showed CT scan signs of acute COVID-19 during the second episode, worsening for 4 in 7 when comparison available, including a case of pulmonary embolism without sign of superinfection and no differential diagnosis (supplementary Table). A SARS-CoV-2 serology was available after D21 for nine patients: five were positive, one slightly positive and three negative. A viral culture was performed on Vero E6 cells from naso-pharyngeal swabs of two patients during the second episode; one was positive with a typical cytopathic effect of SARS-CoV-2 and confirmed by RT-PCR; after sequencing, the strain was shown to belong to the B2 European lineage (Rambaut et al., bioRxiv preprint, doi: https://doi.org/10.1101/2020.04.17.046086).

Immunity to SARS-CoV-2 involves both cell-mediated and humoral responses, but its protective role from re-infection along with definitive viral clearance is uncertain.[7] Our case series of 11 patients having experienced two separate symptomatic COVID-19 episodes, associated with viral detection and no evidence for a differential diagnosis, raises two pathophysiological hypotheses underlying these recurrences: viral reinfection or viral reactivation from sanctuaries. In the case of healthy healthcare workers with mild symptoms at both episodes, a re-infection due to the prolonged exposition can be supposed, given the fact that the immune response may faint in this young population with no invasive infection.[8] The second group included vulnerable persons less likely to have met the virus again and having presented two repeated episodes of hypoxemic pneumonia, fatal in three cases. Recurrence might have occurred due to a suboptimal control of the SARS-CoV-2 infection, allowing a second episode of viral replication.

COVID-19 recurrences should be differentiated from secondary complications such as pulmonary embolism or super infection[5] or persistence of traces of viral RNA that can be detected in respiratory samples up to 6 weeks after onset of symptoms in clinically-cured patients.[9]

Immunosuppressive factors such as drugs or pathological conditions could contribute to impair viral clearance and favour SARS-CoV-2 reactivation.[10] Three of the 7 severe patients of our series, and 3 of 4 patients reported by Ye[3] received corticosteroids during the first episode. Furthermore, from our 3 patients who developed no SARS-CoV-2 antibodies more than 21 days after severe symptoms, two received recent chemotherapy and/or rituximab.

An inflammatory rebound triggered by an inappropriate immune response could constitute an alternative explanation to the recurrence of clinical symptoms. Yet, the facts that viral RNA was detected in all patients -some of them with low cycle threshold- and that a viral strain could be cultured during the second episode for one of them rather support re-infection or virus replication's rebound.

This work has some limitations. In addition to the limited number of observations, the cure between episodes was only clinically-defined (except for patient 6) because iterative RT-PCR controls were not recommended by French guidelines. Finally, viral culture could be performed only for two patients, with no phylogenic sequence comparison at this time.

In conclusion, the fact that patients could experience reactivation of a long-lasting virus carriage or might be re-infected, as well as potential long-term effects of drugs or diseases that

Table 1
Clinical characteristics of COVID 19 first and 2nd episodes, from onset of first episode (D1) to last follow-up (home-care patients: patients1–4; hospitalized patients: patients 5–11).

Patients characteristics				First episode			2nd episode				
Case	Age	Sex	Past medical history	Clinical characteristics	Treatments	1st Clinical cure	2nd ep onset	Clinical characteristics	Treatments	Duration of 2nd episode (days)	Outcome
1	19	F	None (HCW)	FLS with no fever-cough-dyspnoea-AO-DG -headache-diarrhoea-otalgia-	None	D18	D26	FLS-cough-dyspnoea -chest pain	None	on-going	home care
2	32	F	None (HCW)	Cough-AO-myalgia-headache	None	D29	D36	FLS	None	10	cured
3	33	F	First trimester pregnancy (HCW)	Myalgia-headache-fatigue-nasal congestion-sore throat	None	D13	D27	Fatigue-nasal congestion-sore throat-chills	None	8	cured
4	43	M	None (HCW)	FLS-AO- headache	None	D14	D24	Cough-AO-myalgia headache-diarrhoea-fatigue	None	29	cured
5	85	M	Bronchiectasis - CHD - pace maker - arrhythmia	Fever-cough-dyspnoea-fatigue-confusion-falls	O2, ATB	D17	D44	Cough-dyspnoea-fatigue-chest pain-confusion-acute heart failure	O2	6	cured
6	54	M	HT	Fever-cough-dyspnoea -severe ARDS-fatigue	ICU, OTI, ATB, LPV/rtv, CTS	D41	D45	Cough-dyspnoea-diarrhoea-ARDS-fatigue	ICU, OTI, ECMO, ATB	34	death
7	91	F	CHD - HT-CVD-atherosclerosis-arrhythmia- DM	Fever-dyspnoea-fatigue-pleural & pericardial effusion	O2, ATB, CTS	D13	D25	Dyspnoea-fatigue	none	9	cured
8	55	M	CLD, cirrhosis Child C	Fever-headache-fatigue	ATB	D21	D27	Dyspnoea-headache-diarrhoea -fatigue	ICU-HFNIV-OTI ATB	20	cured
9	72	M	Anti MAG neuropathy (rituximab, bendamustine)	Fever- cough-dyspnoea-worsening neuropathy	O2, ATB	D21	D27	Fever- cough- dyspnoea -fatigue – worsening neuropathy	ICU-HFNIV-OTI, ATB remdesivir	29	death
10	73	M	DLBCL (chemotherapy D-22)	Fever-fatigue-abdominal cutaneous rash	ATB	D13	D24	Fever-dyspnoea-fatigue	O2, ATB, CTS *	17	cured
11	84	F	CLD / O2T – mild CRD - CHD arrhythmia/ATC - valvulopathy - atherosclerosis - DM	Fever-cough-dyspnoea-AO-fatigue	O2, curative ATC, ATB + CTS	D23	D49	Fever-cough-dyspnoea-fatigue	O2, HFNIV, ATB,tocilizumab, CTS curative ATC	30	death

Abbreviations : ATB : antibiotics - AO : anosmia – ATC : anticoagulation - CHD : Chronic Heart Disease- CLD : Chronic Lung Disease- CRD : Chronic Renal Disease – CVD : CerebroVascular Disease – CTS : corticosteroids DM : Diabetes Mellitus – DG : dysgeusia - DLBCL : Diffuse Large B Cell Lymphoma – ECMO : extra-corporeal membrane oxygenation – FLS : Flu Like Syndrome (= fever + myalgia + fatigue +/- sore throat, nasal congestion) - HT : hypertension – HCW : Health Care Worker - HFNIV: High Flow Non Invasive Ventilation - ICU : Intensive Care Unit -LPV/rtv : lopinavir/ritonavir – NA : Non Available - OTI : Oro-Tracheal Intubation – O2 : oxygen therapy.

* No improvement after 7 days of piperacillin-tazobactam ; apyrexia 4 days after pip-taz stop and before linezolid.

Table 2
Laboratory findings of COVID 19 first and 2nd episodes, from onset of first episode (D1) to last follow-up.
(home-care patients: patients1–4; hospitalized patients: patients 5–11).

	First episode (onset = D1)			No symptom Minimal CRP Maximal L PCR if available	2nd episode				
Case	Blood tests	SARS CoV2 PCR			Blood tests	SARS CoV2 PCR		Serology	
		Days from onset	CT if available *			Days from 1st onset	CT if available *	Days from 1st onset	Results
1	NA	D2	E 18 - N22 - RdRP 19	NA	NA	D29	E 35 - IP2 37 - IP4 42	D58	POSITIVE total Ig
2	NA	D18	E 23,9- N NA - RdRP 23,6	NA	NA	D36 D55	E 31,5- N NA - RdRP 30,3 NEGATIVE	NA	NA
3	NA	D3	30,5	NA	L 1800	D28	32,7	D27	POSITIVE IgG IgM
4	NA	D3	POSITIVE, CT NA	NA	L 1300 Eo 90CRP 1	D38	21.5	D31, 45	slighly POSITIVE IgG, NEGATIVE IgM
5	L 290 Eo 0 CRP 33	D1	E8 - N11- RdRP 12	L 870 CRP 17 PCR D36 : + E35	L700 Eo 30 CRP 15	D46	E 33 - N 33 - RdRP 32 Viral culture NEGATIVE	NA	NA
6	L 690 CRP 365	D16 D 38, 44	IP2 29,4 - IP4 29.9 NEGATIVE	L 2750 CRP 28	L 690 Eo 50 CRP 247	D45	IP2 38.3 - IP4 36.2	D31	POSITIVE IgG IgM
7	L 720 Eo 10 CRP 143	D3	ORF1 18.7 - N 18.1	L 1500 CRP 34	L 1000 Eo 160 CRP 188	D26	ORF1 29,7	D27	POSITIVE IgG IgM
8	L 629 Eo 0 CRP 74	D6	16	L 1400 CRP 33	L 800 Eo 10 CRP 73	D31	POSITIVE, CT NA	D27 D47	Ambiguous POSITIVE IgG
9	L 630 Eo 260 CRP 39	D7	POSITIVE, CT NA	L 750 Eo 90 CRP 8	L 360 Eo 0 CRP 85	D 23, 32, 36	POSITIVE, CT NA	D41	NEGATIVE
10	L 60 Eo 0 CRP 112.8	D6	17 Cutaneous PCR neg	L 80 CRP 18	L 60 Eo 30 CRP 160	D35	18	D25	NEGATIVE
11	L 770 CRP 88	D11	IP4 31	L 1180 CRP 4.2	L 480 CRP 346	D50	IP4 16,7 Viral culture POSITIVE	D53	NEGATIVE

L : lymphocytes (per mm^3)– Eo = Eosinophils polymorphonuclar leukocytes (per mm^3). CRP : C Reactive Protein (mg/l) NA: Non Available.
* SARS CoV2 Polymerase Chain Reaction: cycle threshold (CT), envelope gene (E), nucleocapsid gene (N), ARN polymerase gene (RdRP, IP2, IP4), specific Open Reading Frame (ORF)1.

hamper the immune response, constitutes a substantial point of vigilance for the management of the pandemic at the individual and collective levels. Studies including genomic comparisons of viral strains involved in both episodes, determination of RNA infectivity by viral culture, as well as assessment of innate and adaptive immunity and monitoring inflammatory targets, would be of great value for further understanding the underlying pathophysiology of these COVID-19 recurrences.

Declaration of Competing Interest

None of the authors has any conflict of interest to declare regarding this subject. This work had no financial support.

Acknowledgements

We thank Mr. Nicolas Dumesges and Mrs Alison Mac Lean for the proofreading.

Supplementary materials

Supplementary material associated with this article can be found, in the online version, at doi:10.1016/j.jinf.2020.06.073.

References

1. Kiyuka P.K., Agoti C.N., Munywoki P.K., Njeru R., Bett A., Otieno J.R., et al. Human Coronavirus NL63 Molecular Epidemiology and Evolutionary Patterns in Rural Coastal Kenya. *J Infect Dis* 2018;**217**(11):1728–39 05.
2. Tang F., Quan Y., Xin Z.-T., Wrammert J., Ma M.-J., Lv H., et al. Lack of peripheral memory B cell responses in recovered patients with severe acute respiratory syndrome: a six-year follow-up study. *J Immunol Baltim Md 1950* 2011;**186**(12):7264–8 Jun 15.
3. Ye G., Pan Z., Pan Y., Deng Q., Chen L., Li J., et al. Clinical characteristics of severe acute respiratory syndrome coronavirus 2 reactivation. *J Infect* 2020;**80**(5):e14–17.
4. Ravioli S., Ochsner H., Lindner G. Reactivation of COVID-19 pneumonia: a report of two cases. *J Infect* 2020 [published online ahead of print, 2020 May 7]. doi:10.1016/j.jinf.2020.05.008.
5. Loconsole D., Passerini F., Palmieri V.O., Centrone F., Sallustio A., Pugliese S., et al. Recurrence of COVID-19 after recovery: a case report from Italy. *Infection* 2020:1–3 [published online ahead of print, 2020 May 16]. doi:10.1007/s15010-020-01444-1.
6. Zhou L., Liu K., Liu H.G. [Cause analysis and treatment strategies of "recurrence" with novel coronavirus pneumonia (COVID-19) patients after discharge from hospital]. Zhonghua Jie He He Hu Xi Za Zhi Zhonghua Jiehe He Huxi Zazhi. *Chin J Tuberc Respir Dis* 2020;**43**(4):281–4 Apr 12.
7. Grifoni A., Weiskopf D., Ramirez S.I., Mateus J., Dan J.M., Moderbacher C.R., et al. Targets of T Cell Responses to SARS-CoV-2 Coronavirus in Humans with COVID-19 Disease and Unexposed Individuals. *Cell* 2020;**181**(7):1489–501 e15. doi:10.1016/j.cell.2020.05.015.
8. Zhao J., Yuan Q., Wang H., Liu W., Liao X., Su Y., et al. Antibody responses to SARS-CoV-2 in patients of novel coronavirus disease 2019. *Clin Infect Dis Off Publ Infect Dis Soc Am [Internet]* 2020. Mar 28 [cited 2020 Jun 26]; Available from http://www.ncbi.nlm.nih.gov/pmc/articles/PMC7184337/ .
9. Xiao A.T., Tong Y.X., Zhang S. Profile of RT-PCR for SARS-CoV-2: a preliminary study from 56 COVID-19 patients. *Clin Infect Dis.* 2020:ciaa460 [published online ahead of print, 2020 Apr 19]. doi:10.1093/cid/ciaa460.
10. Ling Y., Xu S.-B., Lin Y.-X., Tian D., Zhu Z.-Q., Dai F.-H., et al. Persistence and clearance of viral RNA in 2019 novel coronavirus disease rehabilitation patients. *Chin Med J (Engl)* 2020;**133**(9):1039–43 May 5.

Marie Gousseff*[1]
Service de Medecine interne, Maladies Infectieuses, hematologie, Centre Hospitalier Bretagne Atlantique, 20, boulevard Maurice Guillaudot, 56000 Vannes, France

Pauline Penot[1]
Hôpital intercommunal André Grégoire, groupement hospitalier Grand Paris Nord Est, 56, boulevard de la Boissière, 93100 Montreuil, France

Laure Gallay[1]
Service Médecine Interne, Pr Hot, INMG CNRS UMR5310 INSERM U1217, Place d'arsonvaal, 69003 Lyon, France

Dominique Batisse[1]
Department of Infectious Diseases and Immunology, Cochin-Hôtel-Dieu Hospital, Publique –Hôpitaux de Paris (APHP), University of Paris. 1, place parvis Notre Dame, 75014 Paris, France

Nicolas Benech[1]
Service des Maladies Infectieuses et Tropicales, Hôpital de La Croix-Rousse, Hospices Civils de Lyon, 103, Grande Rue de La Croix-Rousse, 69004 Lyon, France

Kevin Bouiller[1]
Department of infectious disease, University Hospital of Besançon, F-25000 Besançon, France
UMR-CNRS 6249 Chrono-environnement, Université Bourgogne Franche-Comté, 25000 Besançon, France

Rocco Collarino[1]
Service des Maladies infectieuses et tropicales, Assistance publique-hôpitaux de Paris, Centre hospitalier universitaire Bicêtre, 78 rue du général Leclerc, 94270 Le Kremlin-Bicêtre, France

Anne Conrad[1]
Service des Maladies Infectieuses et Tropicales, Hôpital de La Croix-Rousse, Hospices Civils de Lyon, 103, Grande Rue de La Croix-Rousse, 69004 Lyon, France

Dorsaf Slama[1]
Department of Infectious Diseases and Immunology, Cochin-Hôtel-Dieu Hospital, Assistance, Publique –Hôpitaux de Paris (APHP), University of Paris. 1, place parvis Notre Dame, 75014 Paris, France

Cédric Joseph[1]
Service des Maladies Infectieuses et Tropicales, CHU Amiens-Picardie, Place Victor Pauchet 80054 Amiens, France

Adrien Lemaignen[1]
Service de Médecine Interne et Maladies Infectieuses, CHRU de Tours, Hôpital Bretonneau, Université de Tours, 2, Boulevard Tonnellé, 37000 Tours, France

François-Xavier Lescure[1]
AP-HP, Infectious and Tropical Diseases Department, Bichat-Claude Bernard University, Hospital, Paris, France
University of Paris, French Institute for Health and Medical Research (INSERM), IAME, U1137, Team DesCID, Paris, France. 46 rue Henri Huchard, 75018 Paris, France

Bruno Levy[1]
Service de Médecine Intensive et Reanimation Brabois, CHRU Nancy, Pôle Cardio-Médico-Chirurgical, Vandoeuvre-les-Nancy, INSERM U1116, Faculté de Médecine, Vandoeuvre-les-Nancy, and Université de Lorraine, France

Matthieu Mahevas[1]
Service de Médecine Interne, Centre Hospitalier Universitaire Henri-Mondor, Assistance Publique-Hôpitaux de Paris, Université Paris Est Créteil, Créteil, France. IMRB - U955 – INSERM Equipe n°2 "Transfusion et maladies du globule rouge" EFS Île-de-France, Hôpital Henri-Mondor, AP-HP, 51, avenue du Maréchal-de-Lattre-de-Tassigny, 94010 Créteil, France

Bruno Pozzetto[1]
GIMAP (EA 3064), University of Saint-Etienne, University of Lyon, Faculty of Medicine of Saint-Etienne, 42023 cedex 02 Saint-Etienne, France

Nicolas Vignier[1]
Groupe hospitalier Sud Ile de France & INSERM, Institut Pierre Louis d'Épidémiologie et de, Santé Publique (IPLESP), Sorbonne Université, Paris, France, 270 avenue Marc Jacquet, 77 000 Melun, France

Benjamin Wyplosz[1]
Service des Maladies infectieuses et tropicales, Assistance publique-hôpitaux de Paris, Centre hospitalier universitaire Bicêtre, 78 rue du général Leclerc, 94270 Le Kremlin-Bicêtre, France

Dominique Salmon[1]
Department of Infectious Diseases and Immunology, Cochin-Hôtel-Dieu Hospital, Assistance, Publique –Hôpitaux de Paris (APHP), University of Paris. 1, place parvis Notre Dame, 75014 Paris, France

Francois Goehringer*[1]
Service de Maladies Infectieuses et Tropicales, Centre Régional Universitaire de Nancy, Hôpitaux de Brabois, Rue du Morvan, 54511 Vandoeuvre Lés Nancy, France

Elisabeth Botelho-Nevers[1]
Infectious Diseases Department, University Hospital of Saint-Etienne, 42055 cedex 02 Saint-Etienne, GIMAP (EA 3064), France University of Saint-Etienne, University of Lyon, Faculty of Medicine of Saint-Etienne, 42023 cedex 02 Saint-Etienne, France

*Corresponding authors.
E-mail addresses: marie.gousseff@ch-bretagne-atlantique.fr (M. Gousseff), pauline.penot@ght-gpne.fr (P. Penot), laure.gallay@chu-lyon.fr (L. Gallay), nicolas.benech@chu-lyon.fr (N. Benech), kbouiller@chu-besancon.fr (K. Bouiller), rocco.collarino@aphp.fr (R. Collarino), anne.conrad@chu-lyon.fr (A. Conrad), joseph.cedric@chu-amiens.fr (C. Joseph), adrien.lemaignen@univ-tours.fr (A. Lemaignen), xavier.lescure@aphp.fr (F.-X. Lescure), matthieu.mahevas@aphp.fr (M. Mahevas), bruno.pozzetto@chu-st-etienne.fr (B. Pozzetto), Benjamin.wyplosz@aphp.fr (B. Wyplosz), Dominique.salmon@aphp.fr (D. Salmon), f.goehringer@chru-nancy.fr (F. Goehringer), elisabeth.botelho-nevers@chu-st-etienne.fr (E. Botelho-Nevers)

[1] all the authors contributed equally to this article.

Accepted 28 June 2020
Available online 30 June 2020

https://doi.org/10.1016/j.jinf.2020.06.073

© 2020 The British Infection Association. Published by Elsevier Ltd. All rights reserved.

Magnetic resonance imaging of COVID-19 anosmic patients reveals abnormalities of the olfactory bulb: Preliminary prospective study

Dear Editor,

We recently read the paper entitled "Self-reported loss of smell without nasal obstruction to identify COVID-19. The multicenter CORANOSMIA cohort study.[1] " Loss of smell without nasal obstruction was commonly found in the coronavirus disease 2019 (COVID-19), accounting for more than 50% of Western patients.[2] The main suspected etiological mechanism consists of the virus spread through the neuroepithelium of the olfactory cleft and a related neuronal cell destruction. However, this mechanism has not been extensively studied through magnetic resonance imaging (MRI) findings on cohort of anosmic COVID-19 patients. In this preliminary study, we investigated the olfactory bulb of COVID-19 patients with or without loss of smell through MRI and we develop a MRI approach to assess the impairment of olfactory bulb.

Adults with laboratory-confirmed COVID-19 diagnosis and self-reported sudden-onset total loss of smell (SOLS) were recruited through the French public call of the COVID-19 Task Force of YO-IFOS (IRB: IJB-0M011–3137). Electronic informed consent was obtained for each patient. The details about the diagnosis procedure were reported in a previous publication.[3] The study was conducted according to the 'Strengthening the Reporting of Observational Studies in Epidemiology (STROBE)' Statement. Clinical and epidemiological characteristics were electronically collected through an online standardized questionnaire developed with Professional Survey Monkey® (San Mateo, California, USA). The olfactory and gustatory features were investigated through the smell and taste component of the National Health and Nutrition Examination Survey (NHNES).[4] Patients benefited from objective olfactory testing (Sniffin'Sticks tests; Medisense, Groningen, Netherlands), which is a validated test allowing categorization of patients into normosmic (16–12), hyposmic (11–9), and anosmic (8–0).[3]

Imaging studies were conducted on a 3-Tesla MR imaging system (MR750; GE Healthcare, Milwaukee, WI, USA) with a 20-channel head and neck coil following a protocol including, in order to assess the olfactory bulb signal, a 3D-FLAIR sequence and a 3D-T2 sequence centered on the olfactory bulbs (OB). The 3D-FLAIR sequence was acquired in coronal plane with the following parameters: TR/TE, 8000/133 ms; TSE factor 80; bandwidth, 120 Hz/pixel; section thickness, 2 mm; matrix 240×240; FOV, $230 \times 230 \times 20$; voxel size, $0.95 \times 0.95 \times 2$ mm; ETL=220 with variable flip angle; acquisition time=4min36sec; imaging option: Fat Sat, T2 prep. Sec-

Table 1
Clinical and epidemiological features of patients.

Characteristics	Patients (N-%)
Age (Mean - SD) - yo	39.0 ± 17.1
Gender (Female/Male)	14/9
Smoker	5 (21.7)
Patients with seasonal allergy	3 (13.0)
Comorbidities	
Hypertension	2 (8.7)
Depression	2 (8.7)
Asthma	2 (8.7)
Hypothyroidism	1 (4.3)
Diabetes	1 (4.3)
Heart problems	1 (4.3)
Neurological diseases	1 (4.3)
Autoimmun disease	1 (4.3)
Hypercholesterolemia	1 (4.3)
General Symptoms (N -%)	
Asthenia	21(91.3)
Headache	18 (78.3)
Cough	17 (73.9)
Fever (>38C)	15 (65.2)
Myalgia	14 (60.9)
Loss of appetite	12 (52.2)
Arthralgia	10 (43.5)
Chest pain	9 (39.1)
Dyspnea	5 (21.7)
Diarrhea	5 (21.7)
Abdominal pain	2 (8.7)
Conjonctivitis	2 (8.7)
Ear, nose and throat Sympotms (N -%)	
Postnasal drip	21 (91.3)
Taste dysfunction	21 (91.3)
Presumed anosmia	19 (82.6)
Nasal obstruction	18 (78.3)
Ear pain	18 (78.3)
Rhinorrhea	17 (73.9)
Face pain/heaviness	16 (69.6)
Throat sputum	12 (52.2)
Sore throat	6 (26.1)
Presumed hyposmia	4 (17.4)
Dysphagia	2 (8.7)

Abbreviations: SD=standard deviation.

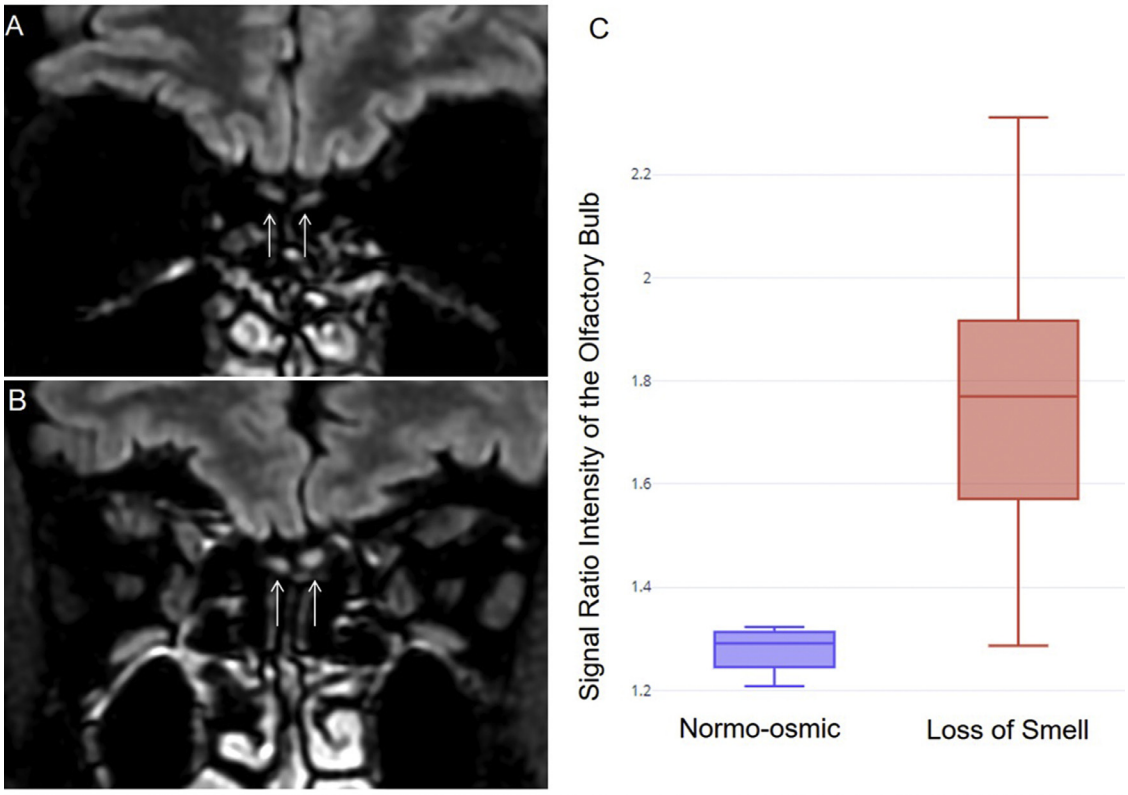

Fig. 1. MRI findings.
Comparison of T2/FLAIR coronal views centered on the olfactory bulbs showing normal signal in a normosmic (A) and T2/FLAIR hyperintensity of the olfactory bulbs in a patient with anosmia (B). Box plot (C) of signal intensity ratio in loss of smell and in normo-osmic group, revealing a statistically higher T2/FLAIR Signal Intensity Ratio of the olfactory bulb in the loss of smell group ($p<0.001$).

tions were angled perpendicular to the anterior base of the skull or cribriform plate. Two experienced neuroradiologists independently performed image analyses. A third neuroradiologist resolved potential discordances. Radiologists were blinded regarding the patient olfactory evaluation (anosmic *versus* normosmic). Qualitative analysis reported the visual analysis of presence of T2/FLAIR OB hyperintensity compared with the signal intensity of the adjacent frontal white matter. Quantitative analysis was performed on T2/FLAIR image by adjusting contours of a ROI centered on the OB on a coronal plane, in order to measure the average OB signal intensity. A signal intensity ratio (SIR) was then calculated between the average signal of the OB and the average signal of a ROI placed in ipsilateral frontal white matter. Statistical analyses were performed using SPSS (version 22.0; IBM Corp, Armonk, NY, USA) according to two subgroups of patients: COVID-19 patients with SOLS and COVID19 without olfactory dysfunction (controls). An intra-class correlation coefficient was performed to compare the reproducibility of signal intensity ratio between two readers. The group outcomes were compared with Mann-Whitney U test.

At the end of the recruitment process, 23 patients were included (14 females). A total of 19 patients composed the SOLS group, while 4 patients did not have anosmia. The clinical and epidemiological characteristics are reported in Table 1. The most common symptoms developed over the disease were: asthenia, headache and cough. The mean duration of symptoms was 9.6 ± 6.9 days. Patients had normal neurological and general examinations. The fiberoptic was not performed because sanitary recommendations. Regarding the NHNES questions, the loss of smell developed after ($N=12$; 63%) the onset of the general symptoms. Taste disorder, which was defined as abnormal sensations of salty, sweet, bitter and sour, was present in 91.3% of patients. The mean sniffin-sticks test was 3.2 ± 4.4. On the 4 patients of the normosmic group (sniffin-sticks test>11), MRI findings reported no abnormal FLAIR hyperintensity of the OB and one patient presented bilateral obstruction of the olfactory cleft.

On the 19 patients with SOLS at the time of the MRI, 9 (47%) presented bilateral obstruction of the olfactory clefts. Statistical analysis of Signal Intensity Ratio of the OB showed significant differences between the SOLS group (mean=1.73±0.23) and the normosmic group (mean=1.27±0.04; $p<0.0001$). The intra-class correlation coefficient for Signal Intensity Ratio measurements was very high (rho=0.94, 95%CI [0.90–0.96], $p<0.001$). Representative cases are reported in Fig. 1.

The present study is the first case-series that describes MRI olfactory abnormalities in COVID-19 patients with SOLS. Three patient profiles were observed: 1) patients with SOLS, OB signal abnormalities (ratio) and no olfactory cleft edema, 2) patients with SOLS, OB signal abnormalities and olfactory cleft edema; and 3) patients without SOLS and normal OB signal. In some cases, the occurrence of concomitant edema of the olfactory cleft mucosa was noted, mainly in the anosmic group but also in one normosmic patient. This could be due to the initial inflammatory reaction of the nasal mucosa since we observed in previous study that mild-to-moderate COVID19 patients with anosmia would have an otolaryngological clinical picture of the disease.[2] These findings support that SOLS could be due to a virus-related inflammatory reaction into the OB, which could impair olfactory neural or sustentacullar cells. The inflammatory reaction could start in the neuroepithelium of the olfactory cleft, which appeared obstructed at the MRI over the first day of SOLS.

The originality of the present work is the development of a quantitative approach of the OB of COVID-19 patients. The ratio analysis is easy to analyze the OB involvement and provides a quantitative approach to determine the presence of the neurolog-

ical pathology as a qualitative analysis alone of the signal of the olfactory bulb can be difficult to appreciate visually, especially on doubtful cases. Visual appreciation may be influenced by the setting of the window level. To be able to adequately measure signal intensity of such small structures as olfactory bulbs, 3D FLAIR sequences must be optimized in terms of spatial resolution. We therefore preferred a coronal acquisition of the sequence, in order to have a submillimetric 'in plane' resolution. OB neuropathy related to chronic rhinosinusitis have already been described as presence of T2/FLAIR hyperintensity of olfactory bulbs.[5] Presence of MRI OB hyperintensities in acute COVID-19 symptomatic patients suggests a viral neuropathy of the OBs, leading to local inflammatory reaction. The main limitation of this study is the low number of patients in both groups but it was not easy to perform MRI in a context of pandemic.

Declaration of Competing Interest

The authors have no conflicts of interest.

Funding

None.

Data availability

Data are available in the Department of Radiology of AP-HP-Garches Hospital.

Acknowledgment

I. Ducamp for the management of the patient appointment. We also thank Pierre-Frédéric Bourcier for his technical support on the optimization of MR sequence parameters. Florence Toutain, Clément Serpette and all the MRI technicians involved in MRI examinations of COVID-19 patients with neurological symptoms.

References

1. Salmon D., Bartier S., Hautefort C., Nguyen Y., Nevoux J., Hamel A.L., Camhi Y., Canouï-Poitrine F., Verillaud B., Slama D., Haim-Boukobza S., Sourdeau E., Cantin D., Corré A., Bryn A., Etienne N., Rozenberg F., Layese R., Papon J.F., Bequignon E.APHP COVID-19 research collaboration Self-reported loss of smell without nasal obstruction to identify COVID-19. The multicenter CORANOSMIA cohort study. *J Infect* 2020 Jul 7 S0163-4453(20)30463-1. doi:10.1016/j.jinf.2020.07.005.
2. Lechien J.R., Chiesa-Estomba C.M., Hans S., et al. Loss of Smell and Taste in 2,013 European Mild-to-Moderation COVID-19 Patients. *Ann Int Med* 2020. doi:10.7326/M20-2428.
3. Lechien J.R., Cabaraux P., Chiesa-Estomba C.M., et al. Objective olfactory evaluation of self-reported loss of smell in a case series of 86 COVID-19 patients. *Head Neck* 2020. doi:10.1002/hed.26279.
4. Rawal S., Hoffman H.J., Bainbridge K.E., Huedo-Medina T.B., Duffy V.B. Prevalence and Risk Factors of Self-Reported Smell and Taste Alterations: results from the 2011-2012 US National Health and Nutrition Examination Survey (NHANES). *Chem Sens* 2016;**41**(1):69–76. doi:10.1093/chemse/bjv057.
5. Chung M.S., Choi W.R., Jeong H.Y., Lee J.H., Kim J.H. MR imaging-based evaluations of olfactory bulb atrophy in patients with olfactory dysfunction. *AJNR Am J Neuroradiol.* 2018;**39**(3):532–7. doi:10.3174/ajnr.A5491.

Annaelle Chetrit[1]
Department of Radiology, APHP, Hôpitaux R. Poincaré-Ambroise Paré, DMU Smart Imaging, GH Université Paris-Saclay, U 1179 UVSQ/Paris-Saclay, Paris, France

Jerome R. Lechien*[1]
Department of Otolaryngology-Head & Neck Surgery, Hopital Foch, Paris Saclay University, UFR Simone Veil, Université Versailles Saint-Quentin-en-Yvelines (Paris Saclay University), Paris, France
Department of Otolaryngology-Head & Neck Surgery, CHU Saint-Pierre (CHU de Bruxelles), Université Libre de Bruxelles, Brussels, Belgium
Department of Human Anatomy and Experimental Oncology, UMONS Research Institute for Health Sciences and Technology, University of Mons (UMons), Mons, Belgium

Amine Ammar
Department of Radiology, APHP, Hôpitaux R. Poincaré-Ambroise Paré, DMU Smart Imaging, GH Université Paris-Saclay, U 1179 UVSQ/Paris-Saclay, Paris, France

Younes Chekkoury-Idrissi, Lea Distinguin, Marta Circiu
Department of Otolaryngology-Head & Neck Surgery, Hopital Foch, Paris Saclay University, UFR Simone Veil, Université Versailles Saint-Quentin-en-Yvelines (Paris Saclay University), Paris, France

Sven Saussez
Department of Otolaryngology-Head & Neck Surgery, CHU Saint-Pierre (CHU de Bruxelles), Université Libre de Bruxelles, Brussels, Belgium
Department of Human Anatomy and Experimental Oncology, UMONS Research Institute for Health Sciences and Technology, University of Mons (UMons), Mons, Belgium

Marie-Christine Ballester
Department of Emergency, Hopital Foch, Paris Saclay University, Paris, France

Marc Vasse
Department of Biology, Hopital Foch, Paris Saclay University, Paris, France

Najete Berradja
Department of Radiology, APHP, Hôpitaux R. Poincaré-Ambroise Paré, DMU Smart Imaging, GH Université Paris-Saclay, U 1179 UVSQ/Paris-Saclay, Paris, France

Stephane Hans[1]
Department of Otolaryngology-Head & Neck Surgery, Hopital Foch, Paris Saclay University, UFR Simone Veil, Université Versailles Saint-Quentin-en-Yvelines (Paris Saclay University), Paris, France

Robert Carlier[1]
Department of Radiology, APHP, Hôpitaux R. Poincaré-Ambroise Paré, DMU Smart Imaging, GH Université Paris-Saclay, U 1179 UVSQ/Paris-Saclay, Paris, France

Myriam Edjlali[1]
Department of Radiology, APHP, Hôpitaux R. Poincaré-Ambroise Paré, DMU Smart Imaging, GH Université Paris-Saclay, U 1179 UVSQ/Paris-Saclay, Paris, France
Department of Neuroradiology, Université Paris-Descartes-Sorbonne-Paris-Cité, IMABRAIN-INSERM-UMR1266, DHU-Neurovasc, Centre Hospitalier Sainte-Anne, Paris, France

*Corresponding author at: Department of Otolaryngology-Head & Neck Surgery, Hopital Foch, Paris Saclay University, UFR Simone Veil, Université Versailles Saint-Quentin-en-Yvelines (Paris Saclay University), Paris, France.
E-mail address: Jerome.Lechien@umons.ac.be (J.R. Lechien)

[1] These authors contributed equally to this work.

Accepted 27 July 2020
Available online 30 July 2020

https://doi.org/10.1016/j.jinf.2020.07.028

© 2020 The British Infection Association. Published by Elsevier Ltd. All rights reserved.

SARS-CoV-2 IGM and IGG rapid serologic test for the diagnosis of COVID-19 in the emergency department

Dear Editor,

We read with interest the article by Pan et al.[1] on the performance of a serological immunochromatographic assay for SARS-CoV-2 diagnosis. As discussed by the authors, there is an urgent need for rapid tests for SARS-CoV-2 in the supplement to the current diagnosis. The gold standard is the molecular testing of upper or lower respiratory tract samples by reverse transcription polymerase chain reaction (RT-PCR),[2] which suffers from several limitations[3]: long turnaround times and up to 30% of false negatives, due to technical errors and time sampling.[4,5] The serologic assays to detect antibodies against SARS-CoV-2 are of great interest[6] as high levels of IgM and IgG can be detected from the second week of symptom's onset, although IgM can be positive from the fourth day and IgG after 8 days.[3,6] In the French emergency departments (ED) there was a rising number of suspected cases of COVID-19 from mid-march and a huge effort was made in order to isolate these suspected patients to avoid hospital SARS-CoV spread and transmission. Molecular tests and classic serology immunoassays have a relatively long turnaround times, which are not suitable for EDs to take fast disposition decisions. The recent development of rapid antibody detection tests for Sars-CoV2 (lateral flow immunoassay, LFI) can be very useful in this context.

The present study collected prospective data of 164 patients admitted in April 2020 to the ED of two academic hospitals in Paris, France, if: 1) COVID-19 was suspected on presenting symptoms and 2) a nasopharyngeal swab was prescribed for SARS-CoV-2 RT-PCR. Waived inform consent was obtained because of the routine care design. The LFI used for evaluation was SGTi-flex COVID-19 IgM/IgG (Sugentech, republic of Korea) which is a nanoparticle-based immunochromatographic test kit for qualitative determination of COVID-19′s IgM and IgG antibodies in human whole blood (finger prick or venous), serum or plasma. The results can be observed within 10 min after applying the sample and 3 drops of diluent. At the same time of first ED blood collection, a sample was also drawn in parallel for SARS-CoV-2 IgG detection with a chemiluminescent microparticle immunoassay (CMIA) in serum (Abbott Architect).

Seven patients were excluded because the result of either RT-PCR or LFI missed. The 157 remaining patients were divided in two groups according to the SARS-CoV-2 RT-PCR test results: positive or negative.

Table 1 shows the demographic characteristics, symptoms, laboratory and imaging test results in the ED. There were 20 (13%) patients tested positive for SARS-CoV-2 RT-PCR, of which 15 (75%) were positive for the LFI (2 for IgM, 3 for IgG and 10 for IgM + IgG) and 5 (25%) tested negative (Table 2). Among the 13 patients for whom the LFI showed an IgG band, 12 had IgG detected by CMIA. Three of the RT-PCR ±/LFI- patients had their first symptoms in the 7 days and the 2 last before 14 days. These 5 false negative LFI were explained by either too early tests, a low antibody level below the detection limit of this LFI, or the immune response variability in individual antibodies production.[3]

Among the 137 patients who tested negative for RT-PCR, there were 27 (20%) with a positive LFI, of whom 16 (59%) exhibited an IgM band, 4 (15%) an IgG band and 7 (26%) both bands. Among the 42 positive LFI, 18 (42.8%) were positive for IgM with symptoms onset varying from 0 to 21 days; 7 (16.7%) were positive for IgG, all with symptom's onset within the first 7 days; and 17 (40.5%) were positive for both, with symptoms onset varying from 0 to 30 days (9 had first symptoms in 7 days and 4 between 7 and 14 days).

Concordance between LFI and CMIA IgG calculated on 155 samples with conclusive results was 94.8% Globally, in these 157 suspected COVID-19 cases attending the ED, LFI had (Table 2) a sensitivity of 75% [95% CI 69.5–80.5], specificity 80.3% [95% CI 75,2–85,4], positive predictive value 35.7% [95% CI 29.6–41.8] and nega-

Table 1
Emergency Department's patient's characteristics according to group (RT-PCR positive or negative).

Characteristics	Total ($n=157$)	RT-PCR negative ($n=137$)	RT-PCR positive ($n=20$)
Sex			
Male	83 (52.9%)	74 (46%)	9 (45%)
Female	74 (47.1%)	63 (54%)	11 (55%)
Median	70	71	62.00
Age (years)	(54–80)	(54–81)	(52.5–75.8)
Symptoms onset			
0–7 days	115 (73.3%)	101 (73.7%)	14 (70%)
8–14 days	16 (10.2%)	12 (8.8%)	4 (20%)
15–21 days	14 (8.9%)	12 (8.8%)	2 (10%)
> 21 days	12 (7.6%)	12 (8.8%)	0 (0%)
Symptoms			
Fever	39 (24.8%)	32 (23.4%)	7 (35%)
Cough	57 (36.3%)	45 (32.8%)	12 (60%)
Myalgia	17 (10.8%)	12 (8.8%)	5 (25%)
Dyspnea	68 (43.3%)	57 (41.6%)	11 (55%)
Chest pain	39 (24.8%)	34 (24.8%)	5 (25%)
Diarrhea	22(14%)	20 (14.6%)	2 (10%)
Vomiting	25 (15.9%)	23 (16.8%)	2 (10%)
Ageusia	6 (3.8%)	5 (3.6%)	1 (5%)
Anosmia	5 (3.2%)	3 (2.2%)	2 (10%)
Asthenia	40 (25.5%)	36 (26.3%)	4 (20%)
Falling	11 (7%)	11 (8%)	0 (0%)
Headache	21 (13.4%)	16 (11.7%)	5 (25%)
Chest CT scan	106 (67,51%)	90 (65.7%)	16 (80%)
Chest CT scan evocative COVID-19	$n=106$	$n=90$	$n=16$
	26 (24.5%)	15 (16.7%)	11 (68.8%)
Median Leucocytes (Giga/L)	8.33	8.33	8.46
	(6.44–10.85)	(6.46–11.15)	(5.35–9.59)
Lymphocytes (Giga/L)	1,31	1,27	1,79
	(0.88–1.78)	(0.83–1.59)	(1.27–2.21)
Protein-C-reactive (mg/L)	16	16	27.5
	(3–54)	(3–54)	(14–71.1)

Table 2
Comparison of SARS-CoV-2 RT-PCR and LFI's results .

		RT-PCR		Rapid IgM/IgG	
		Positive	Negative	Sensitivity (95% CI)	75% (69.5–80.5)
LFI IgM/IgG	Positive	15	27	Specificity (95% CI)	80.3% (75.2–85.4)
	Negative	5	110	Positive predictive value (95% CI)	35.7% (29.6–41.8)
	Total	20	137	Negative predictive value (95% CI)	95.7% (93.1–98.3)

tive predictive value 95,7% [95% CI 93.1–98.3], compared to RT-PCR as the gold standard.

Cassaniti et al.[7] compared a rapid IgM/IgG test with RT-PCR in the ED and reported that 8.3% exhibited a positive result for IgM/IgG LFI while RT-PCR was negative. Other studies found similar rates of 11%,[8] which are slightly lower than our results but still suggesting an added value of LFI to identify some COVID-19 positive patients with negative RT-PCR.

There are few peer-reviewed publications that have reported the accuracy of COVID-19 diagnostic results obtained by LFI with respect to RT-PCR tests.[3,7–10] Sensibility and specificity varied from a study to another: Li et al. found 88.66% and 90.63%, respectively while Shen et al. found 71.1% and 96.2%.[3,10] In our study the sensitivity and specificity are slightly lower than what was described by previous studies and that's the reason why we recommend to use LFI together with RT-PCR in order to have the lowest false negative's number of patients.

In conclusion, although LFIs cannot confirm the virus presence and replace RT-PCR, they may be sensitive and specific enough to be used as a complementary assay to the existing RT-PCR in the ED. It has the advantage, in comparison with RT-PCR, of saving time without necessitating any extensive equipment; it is simple to use and requiring minimal training.

From our point of view, LFIs should be used in the ED as a complementary assay to the existing SARS-Cov-2 RT-PCR, to better and quicker qualify COVID-19 patients.

References

1. Pan Y., Li Xinran, Yanga G., Fana J., Tanga Y., Zhaoa J., Longa X., Guoa S., Zhaoa Z., Liua Y., Hua H., Xuea H., Li Y. Serological immunochromatographic approach in diagnosis with SARS-CoV-2 infected COVID-19 patients. *J Infect* Jul 2020;**81**(1) e28–e32.
2. Theel E.S., Slev P., Wheeler S., Couturier M.R., Wong S.J., Kadkhoda K. The Role of Antibody Testing for SARS-CoV-2: is There One? *J Clin Microbiol. J Clin Microbiol. [Preprint]* 2020;**29** AprilAvailable from: https://doi.org/10.1128/JCM.00797-20.
3. Li Z., Yi Y., Luo X., Xiong N., Liu Y., Li S., Sun R., Wang Y., Hu B., Chen W., Zhang Y., Wang J., Huang B., Lin Y., Yang J., Cai W., Wang X., Cheng J., Chen Z., Sun K., Pan W., Zhan Z., Chen L., Ye F. Development and clinical application of a rapid IgM-IgG combined antibody test for SARS-CoV-2 infection diagnosis. *J Med Virol [Preprint].* 2020 Feb 27Available from: https://doi.org/10.1002/jmv.25727.
4. Xiao A.T., Tong Y.X., Zhang S. False-negative of RT-PCR and prolonged nucleic acid conversion in COVID-19: rather than recurrence. *J Med Virol [Preprint].* 2020 April 9,Available from: http://doi.org/10.1002/jmv.25855.
5. Long C., Xu H., Shen Q., Zhang X., Fan B., Wang C., Zeng B., Li Z., Li X., Li H. Diagnosis of the Coronavirus disease (COVID-19): rRT-PCR or CT? *Eur J Radiol* 2020;**126**:108961.
6. Sethuraman N., Jeremiah S.S., Ryo A. Interpreting Diagnostic Tests for SARS-CoV-2. *JAMA [Preprint].* 2020. Mai 6Available from: https://jamanetwork.com/journals/jama/fullarticle/2765837 .
7. Cassaniti I., Novazzi F., Giardina F., Salinaro F., Sachs M., Perlini S., Bruno R., Mojoli F., Baldanti F. Performance of VivaDiag COVID-19 IgM/IgG Rapid Test is inadequate for diagnosis of COVID-19 in acute patients referring to emergency room department. *J Med Virol [Preprint].* 2020 April 8,Available from: http://doi.org/10.1002/jmv.25800.
8. Döhla M., Boesecke C., Schulte B., Diegmann C., Sib E., Richter E., Eschbach-Bludau E., Aldabbagh S., Marx B., Eis-Hübinger A.-.M., Schmithausen R.M., Streeck H. Rapid point-of-care testing for SARS-CoV-2 in a community screening setting shows low sensitivity. *Public Health* 2020;**182** 170-;2.
9. Shen B., Zheng Y., Zhang X., Zhang W., Wang D., Jin J., Lin R., Zhang Y., Zhu G., Zhu H., Li J., Xu J., Ding X., Chen S., Lu R., He Z., Zhao H., Ying L., Zhang C., Lv D., Chen B., Chen J., Zhu J., Hu B., Hong C., Xu X., Chen J., Liu C., Zhou K., Li J., Zhao G., Shen W., Chen C., Shao C., Shen X., Song J., Wang Z., Meng Y., Wang C., Han J., Chen A., Lu D., Qian B., Chen H., Gao H. Clinical evaluation of a rapid colloidal gold immunochromatography assay for SARS-Cov-2 IgM/IgG. *Am J Transl Res* 2020;**12**(4):1348–54.
10. Spicuzza L., Montineri A., Manuele R., Crimi C., Pistorio M.P., Campisi R., Vancheri C., Crimi N. Reliability and usefulness of a rapid IgM-IgG antibody test for the diagnosis of SARS-CoV-2 infection: a preliminary report. *J Infect [Preprint].* 2020 April 23,Available from: https://doi.org/10.1016/j.jinf.2020.04.022.

Marta Cancella de Abreu, Christophe Choquet, Héloise Petit, Donia Bouzid, Florence Damond, Stephane Marot, Valentine Marie Ferre, Sonia Burrel, David Boutolleau, Nadhira Houdou-Fidouh, Anne-Geneviève Marcelin, Diane Descamps, Pierre Hausfater
Emergency Department, Hôpital Pitié-Salpêtrière, 7-83 Boulevard de l'Hôpital, 75013 Paris, France

*Corresponding author.
E-mail address: martabfca@gmail.com (M. Cancella de Abreu)

Accepted 28 July 2020
Available online 30 July 2020

https://doi.org/10.1016/j.jinf.2020.07.032

© 2020 The British Infection Association. Published by Elsevier Ltd. All rights reserved.

In-hospital use of ACEI/ARB is associated with lower risk of mortality and critic illness in COVID-19 patients with hypertension

Dear Editor,

We read with great interest the recent article published by Macro Zuin et al. in this journal suggested the prevalence of hypertension and its contribution to increased mortality risk in COVID-19 patients.[1] RAAS inhibitors is one of the commonly used medication for hypertension management. However, since the culprits of COVID-19, SARS-COV-2, takes advantage of membrane-bound angiotensin-converting enzyme 2 (ACE2) to infect host cells,[2] and which were reported to be upregulated in result of treatment of RAAS inhibitors,[3,4] concerns of using RAAS inhibitors in COVID-19 patients with hypertension were aroused. Nonetheless, in animal models of acute lung injury and other influenza virus infection, ACEI and ARB are protective by inhibiting the downregulation of ACE2 and further limit disease progression.[5,6] Thus, RAAS inhibitors might be theoretically protective in patient with COVID-19. Despite various studies showed that RAAS inhibits were not harmful in COVID-19,[7,8] more clinical data and evidence are needed for clarifying this controversial issue and developing better treatment plans for patients suffering COVID-19.

Here, we present a retrospective study, analyzing use of different antihypertensive drugs and its association with various outcomes of COVID-19 patients with hypertension. Overall, 971 hypertensive patients among 2044 participants discharged or died

Table 1
Odds ratio for variable outcomes of patients who received RAAS inhibitors and those in uncontrol group.

	ACEI/ARB ($N=196$) vs. Uncontrol ($N=233$)		Beta–blocker ($N=248$) vs. Uncontrol ($N=233$)		CCB ($N=589$) vs. Uncontrol ($N=233$)		Diuretics ($N=56$) vs. Uncontrol ($N=233$)	
	OR (95%CI)	*p*	OR (95%CI)	*p*	OR (95%CI)	*p*	OR (95%CI)	*p*
COVID–19 critic, *n*(%)	0.43(0.17–1.06)	**0.080**	0.80(0.40–1.57)	**0.509**	0.84(0.48–1.47)	**0.539**	0.75(0.13–4.51)	**0.755**
Sepsis, *n*(%)	1.29(0.72–2.31)	**0.387**	1.46(0.85–2.51)	**0.171**	1.23(0.79–1.92)	**0.351**	1.27()0.37–4.36	**0.707**
Septic shock, *n*(%)	0.34(0.12–0.99)	**0.047**	0.69(0.34–1.40)	**0.300**	0.85(0.47–1.54)	**0.598**	0.81(0.13–4.90)	**0.821**
Respiratory failure, *n*(%)	0.47(0.16–1.04)	**0.059**	0.75(0.38–1.46)	**0.392**	0.81(0.47–1.40)	**0.444**	0.91(0.18–4.51)	**0.906**
ARDS, *n*(%)	1.07(0.57–2.03)	**0.831**	1.13(0.63–2.03)	**0.670**	1.15(0.70–1.87)	**0.579**	1.57(0.43–5.78)	**0.495**
Heart failure, *n*(%)	0.98(0.36–2.70)	**0.974**	0.92(0.43–2.00)	**0.840**	0.69(0.351.37)	**0.294**	0.66(0.06–7.10)	**0.731**
Coagulopathy, *n*(%)	1.12(0.47–2.67)	**0.805**	0.95(0.50–1.82)	**0.874**	0.97(0.54–1.73)	**0.909**	0.53(0.05–5.23)	**0.589**
Cardiac injury, *n*(%)	1.67(0.84–3.34)	**0.146**	1.59(0.90–2.85)	**0.114**	0.96(0.59–1.56)	**0.871**	2.58(0.68–9.71)	**0.162**
Kidney injury, *n*(%)	0.67(0.31–1.44)	**0.307**	0.62(0.32–1.21)	**0.158**	0.73(0.43–1.22)	**0.229**	0.68(0.015–3.13)	**0.623**
Liver injury, *n*(%)	1.13(0.632.02)	**0.680**	1.06(0.61–1.83)	**0.832**	1.15(0.74–1.80)	**0.534**	0.83(0.23–3.05)	**0.779**
Hypoproteinemia, *n*(%)	0.84(0.44–1.61)	**0.599**	0.89(0.50–1.60)	**0.701**	0.88(0.54–1.44)	**0.616**	0.88(0.21–3.78)	**0.864**
Secondary infection, *n*(%)	3.27(0.23–47.90)	**0.384**	5.32(0.53–53.42)	**0.156**	3.99(0.32–49.07)	**0.279**	___	___
ICU admission, *n*(%)	0.21(0.05–0.99)	**0.049**	0.57(0.25–1.34)	**0.198**	0.85(0.43–1.65)	**0.621**	0.49(0.05–4.91)	**0.543**
Death, *n*(%)	0.26(0.08–0.80)	**0.019**	0.60(0.29–1.24)	**0.167**	0.68(0.38–1.22)	**0.192**	0.31(0.03–3.00)	**0.310**

Abbreviations: ARDS: adult respiratory distress syndrome; ICU, intensive care unit.
"___" The number of cases was too small to analysis.

in two campuses of Tongji hospitals, Wuhan, the Sino-French New City Campus, and the Optical Valley Campus, from January 27th to March 21st were enrolled (Fig. S1).

In this study, 733 (75.49%) patients with hypertension had at least one of the five categories of antihypertensive medications (ACEI, ARB, beta-blocker, CCBs, and diuretic), and 233 (24.51%) patients with hypertension had none of them (Table S1). Among the 733 patients, 27 (3.68%) and 169 (23.06%) patients used ACEIs and ARBs, respectively. CCBs were most used since 589 (80.35%) patients took these agents. 733 patients were classified according to the antihypertensive medications they received. Considering there were 27 cases in ACEI group and use of ACEI and ARB had no substantial difference in all aspects of comparison (Table S2), the two groups were merged into ACEI/ARB (RAAS inhibitors) group for later analysis.

In logistic regression model adjusted by propensity score, use of RAAS inhibitors, beta-blockers, and CCBs showed no significant difference (Table S3). And use of diuretics was associated with higher risk of cardiac injury (OR=2.65, 1.25–5.62, $p=0.011$) vs. use of non-diuretics. Parameters for adjusting were listed in supplementary materials.

To have a more overall estimation, we further compared the risk of various outcomes between 233 patients in uncontrol group, who did not have antihypertensive drugs during hospitalization, and patients in medication group. As shown in Table 1, patients who used beta-blockers, CCBs, and diuretics exhibited no signifi-

Table 2
Various outcomes of patients in ACEI/ARB group and uncontrol group after matching.

	Uncontrol ($N=130$)	ACEI/ARB ($N=130$)	Total ($N=260$)	*p*
Maximum severity of COVID–19 during hospitalization, *n*(%)				
General	59(45.38)	58(44.62)	117(45)	**0.012**
Severe	46(35.38)	62(47.69)	108(41.54)	
Critic	25(19.23)	10(7.69)	35(13.46)	
Maximum of SOFA score, *n*(%)				
0	83(63.85)	75(57.69)	158(60.77)	**0.045**
1	22(16.92)	38(29.23)	60(23.08)	
2	25(19.23)	17(13.08)	42(16.15)	
Maximum of SOFA score	1(0–3)	1(0–2)	1(0–2)	**0.8958**
Onset to ICU, day	12(62–24)	21(18–27)	18.5(9–25)	**02361**
Onset to discharge, day	32(24–39)	35(29–47)	33.5(26–42)	**0.0003**
ICU length, day	8(3–13)	7(6–8)	7.5(3–9)	**0.7283**
Viral duration, day	23.5(17–30.5)	26(19–31)	24(18–31)	**0.1782**
Sepsis, *n*(%)	46(35.38)	53(40.77)	99(38.08)	**0.371**
Septic shock, *n*(%)	20(15.38)	7(5.38)	27(10.38)	**0.008**
Respiratory failure, *n*(%)	26(20.00)	12(9.23)	38(14.62)	**0.014**
ARDS, *n*(%)	33(26.38)	33(25.38)	66(25.38)	**1.000**
Heart failure, *n*(%)	13(10.08)	5(3.85)	18(6.95)	**0.049**
Coagulopathy, *n*(%)	18(13.85)	9(6.92)	27(10.38)	**0.067**
Cardiac injury, *n*(%)	26(22.81)	35(28.93)	61(25.96)	**0.285**
Kidney injury, *n*(%)	25(19.23)	15(11.54)	40(15.38)	**0.086**
Liver injury, *n*(%)	43(33.08)	57(43.85)	100(38.46)	**0.074**
Hypoproteinemia, *n*(%)	35(26.92)	37(28.46)	72(27.69)	**0.782**
Second infection, *n*(%)	0(0.00)	1(0.77)	1(0.38)	**1.000**
ICU admission, *n*(%)	13(10.00)	5(3.85)	18(6.92)	**0.051**
Death, *n*(%)	22(16.92)	6(4.62)	28(10.77)	**0.001**
Hospitalization time of survivals [†], day	18(11–24)	23(16.5–30.5)	20(14–27.5)	**<0.0001**
Hospitalization time of victim[§], day	7.5(5–15)	14(8–19)	8.5(5–17)	**0.0764**
Disease duration of survivals, day	32(25–40)	36(29–47)	35(28–43)	**0.004**
Disease duration of victims, day	21(16–32)	23.5(20–27)	23(16.5–30)	**0.8008**

Abbreviations: SOFA, Sequential Organ Failure Assessment.
[†] Hospitalization time of survivals was defined as the time from admission to hospital to discharge of patients who survived from COVID-19.
[§] Hospitalization time of victim was defined as the time from admission to hospital to death of patients who did not survived from COVID-19.

cant difference compared with uncontrol group. However, patients used RAAS inhibitors had lower risk of death (OR=0.26, 0.08–0.80, $p=0.019$), ICU admission (OR=0.21, 0.05–0.99, $p=0.049$), and septic shock (OR=0.34, 0.12–0.99, $p=0.047$).

Then, we took a closer look at ACEI/ARB group and uncontrol group. These two groups were imbalanced in some baseline characteristics, as shown in Table S4. To eliminate the distractions of confounding factors, we introduced coarsened exact matching to get a proper cohort for further analysis. The matching parameters included age, sex, history of chronic cardiovascular disease, and severity of disease at admission. 130 patients were successfully matched in ACEI/ARB group to uncontrol group at a ratio of 1:1, and baseline characteristics of matched patients were shown in Table S4. The treatments patients received in hospital in two groups were similar in matched groups (Table S5). After matching, results were even more encouraging, use of RAAS inhibitors was associated with remarkably lower mortality (4.62% vs. 16.92%, $p=0.001$) than uncontrol group (Table 2 and Fig. S2). And the rate of septic shock and heart failure were 2.86 times lower (5.38% vs. 15.38%, $p=0.008$) and 2.62 times lower (3.85% vs. 10.08%, $p=0.049$) in ACEI/ARB group than uncontrol group, respectively. As of outcomes of respiratory system, 9.23% of patients in ACEI/ARB group progressed into respiratory failure, by contrast with 20.00% in uncontrol group ($p=0.014$). For ARDS, numbers of case in both groups were 33. As for the highest level of disease severity during patients' hospitalization, 7.69% of patients in AECI/ARB group were classified as critically ill, while 19.23% in uncontrol group ($p=0.012$). And maximum SOFA score of 13.08% of patients were rated as level 2, while 19.23% in uncontrol group ($p=0.045$).

Our retrospective analysis implied that in-hospital use of ACEI/ARB was not substantially associated with higher risk of progressing into unfavorable outcomes. Furthermore, in comparison between patients who received a specific kind of antihypertensive medication and those who did not have any relative drugs administration, ACEI/ARB demonstrated a protective effect, while other three kinds of antihypertensive drugs did not exhibit obvious advantages. Besides, we found that patients in diuretics group had higher risk of cardiac injury than those had other antihypertensive agents administration, after ruling out the use of diuretics for purpose of reducing capacity and took history of cardiovascular disease into propensity score. The mechanism behind this association remained enigmas and needs further assessments.

There are several limitations of this study. First, our cases we collected were primarily Wuhan locals, so impact of races and geographical differences could not be reflected. Second, limited by the nature of retrospective research, medication extracted from electronic system may not match the actual drug use of some patients. Third, we did not take cigarette exposure history, psychological status, education level, and other social factors into analysis, which may impose influence on results.

In summary, despite that confounding factors not taken into analysis might contribute to the positive role ACEI/ARB played, we were confident to reach the conclusion that in-hospital use of ACEI/ARB was protective, instead of harmful, in COVID–19 patients with hypertension.

Declaration of Competing Interest

The authors declare no conflicts of interest.

Ethical approval

The study design was approved by ethics committees of Tongji hospital (TJ-IRB20200406), and the requirement for informed consent was waived by the ethics committees. The trial has been registered in Chinese Clinical Trial Registry (ChiCTR2000032161).

Funding

This study was funded by the National Science and Technology Major Sub-Project (2018ZX10301402–002), the Technical Innovation Special Project of Hubei Province (2018ACA138), the National Natural Science Foundation of China (81772787 and 81974405), and the Fundamental Research Funds for the Central Universities (2019kfyXMBZ024).

Acknowledgment

We are grateful to all health-care workers and people nationwide and worldwide, who are involved in the fighting against COVID-19.

Supplementary materials

Supplementary material associated with this article can be found, in the online version, at doi:10.1016/j.jinf.2020.08.014.

References

1. Zuin M., Rigatelli G., Zuliani G., Rigatelli A., Mazza A., Roncon L. Arterial hypertension and risk of death in patients with COVID-19 infection: systematic review and meta-analysis. *J Infect* 2020;**81**:e84–6.
2. W D., W N., C K.S., G J.A., H C.L., A O., et al. Cryo-EM structure of the 2019-nCoV spike in the prefusion conformation. *Science* 2020;**367**:1260–3 (New York, NY).
3. Ferrario C., Jessup J., Chappell M., Averill D., Brosnihan K., Tallant E., et al. Effect of angiotensin-converting enzyme inhibition and angiotensin II receptor blockers on cardiac angiotensin-converting enzyme 2. *Circulation* 2005;**111**:2605–10.
4. IE S., R A., S B.T., vG H., TM J.M., C J.G.F., et al. Circulating plasma concentrations of angiotensin-converting enzyme 2 in men and women with heart failure and effects of renin-angiotensin-aldosterone inhibitors. *Eur Heart J* 2020;**41**:1810–17.
5. Imai Y., Kuba K., Rao S., Huan Y., Guo F., Guan B., et al. Angiotensin-converting enzyme 2 protects from severe acute lung failure. *Nature* 2005;**436**:112–16.
6. K K., Y I., S R., H G., F G., B G., et al. A crucial role of angiotensin converting enzyme 2 (ACE2) in SARS coronavirus-induced lung injury. *Nat Med* 2005;**11**:875–9.
7. Fosbøl E., Butt J., Østergaard L., Andersson C., Selmer C., Kragholm K., et al. Association of angiotensin-converting enzyme inhibitor or angiotensin receptor blocker use with COVID-19 diagnosis and mortality. *JAMA* 2020. doi:10.1001/jama.2020.11301.
8. Mehta N., Kalra A., Nowacki A.S., Anjewierden S., Han Z., Bhat P., et al. Association of use of angiotensin-converting enzyme inhibitors and angiotensin II receptor blockers with testing positive for coronavirus disease 2019 (COVID-19). *JAMA Cardiology* 2020. doi:10.1001/jamacardio.2020.1855.

Yuan Yuan[1], Dan Liu[1], Shaoqing Zeng[1], Siyuan Wang[1], Sen Xu, Ya Wang, Ruidi Yu, Yue Gao, Huayi Li
National Medical Center for Major Public Health Events, Tongji Hospital, Tongji Medical College, Huazhong University of Science and Technology, 1095 Jiefang Ave, Wuhan 430000, People's Republic of China

Xinxia Feng
Department of Gastroenterology, Tongji Hospital, Tongji Medical College, Huazhong University of Science and Technology, Wuhan 430000, People's Republic of China

Ning Zhou, Chunxia Zhao*
Department of Cardiology, Tongji Hospital, Tongji Medical College, Huazhong University of Science and Technology, 1095 Jie-Fang Avenue, Wuhan, Hubei 430000, People's Republic of China

Qinglei Gao*
National Medical Center for Major Public Health Events, Tongji Hospital, Tongji Medical College, Huazhong University of Science and Technology, 1095 Jiefang Ave, Wuhan 430000, People's Republic of China

*Corresponding authors.
E-mail addresses: zhaocx2001@126.com (C. Zhao), qingleigao@hotmail.com (Q. Gao)

[1] Authors contributed equally to this work.
Accepted 8 August 2020
Available online 12 August 2020

https://doi.org/10.1016/j.jinf.2020.08.014

© 2020 The British Infection Association. Published by Elsevier Ltd. All rights reserved.

Metagenomic sequencing in the management of fungal periprosthetic joint infection

Dear Editor,

We read with interest a recently published article by Zhang HC et al., where metagenomic next-generation sequencing (mNGS) showed promising potential in pathogen diagnosis during focal infections.[1] We also applied mNGS to perform the pathogen diagnosis with periprosthetic joint infections (PJIs), a very common but intractable focal infection in musculoskeletal infection that involves with prosthesis, and found it especially valuable in diagnosis of fungal PJIs. Reportedly accounting for approximately 1% of all PJIs cases, fungal PJI is considered atypical and difficult-to-treat, having a treatment failure rate of over 50%.[2] The delayed or missed identification of fungal pathogens is regarded as a key factor in the failure of treatment. In fungal PJIs, culture has been shown to have a sensitivity as low as 50% and take longer period to get the positive results than bacterial infections.[2] Meanwhile, the current empirical and broad-spectrum antibiotic approach for culture-negative PJIs, was usually able to cover most bacterial pathogens, but not to cover fungal pathogens, which further aggravates the difficulties in fungal PJI management.[3] Hence, timely and accurate diagnosis of fungal pathogens is urgently needed for fungal PJIs, which might enable clinicians to make more timely and targeted therapeutic decisions.

Untargeted mNGS is an unbiased and rapid molecular diagnostic technique, which can theoretically detect all pathogens in a clinical sample with no previous diagnosis hypothesis.[4,5] Based on our previous practice, we found that mNGS had no obvious advantage in the diagnosis of common PJI pathogens, such as *staphylococcus aureus* and coagulase negative staphylococcus. Nevertheless, it showed great value in the detection of rare pathogens, especially fungal pathogens. In the presented prospective study, we firstly reported a series of 8 fungal PJI cases with the assistant diagnosis of mNGS and focused on the application value of mNGS in the management of fungal PJIs.

Between October 2017 and October 2019, at our institution, 8 patients were diagnosed as PJIs with the criteria of the Musculoskeletal Infection Society (MSIS) and further identified as fungal PJIs with the feedback of pathogen detection results. As shown in Table 1, 6 males and 2 females with prosthesis failure (7 knees and 1 hip) were recruited in our study, most of whom had comorbidities such as diabetes or rheumatoid disease and suffered from typical clinical symptoms of infection for weeks or months. Four of them had initial antibiotic treatments before hospitalized. Preoperative and intraoperative pathogen diagnosis revealed 3 of them had mixed infection with fungal and bacterial organisms, while 5 of them had single infection with fungal organism. After prudent consideration, operative treatments were performed for 7 of them, the first stage of two-stage revision (cement spacer implanation) for 6, respectively, debridement and implant retention (DAIR) for 1, respectively, while conservative treatments with antifungal drugs only were decided for the other pa-

Table 1
Patient data, pathogen identification, antibiotic treatment, operative treatment and outcome.

Case number	Patient 1	Patient 2	Patient 3	Patient 4	Patient 5	Patient 6	Patient 7	Patient 8
Gender/age(y)	Male/67	Male/68	Male/44	Male/68	Female/72	Male/56	Female/66	Male/50
Co-morbidities	Hypertension diabetes	Hypertension diabetes	Diabetes	Hypertension diabetes	Hypertension	Diabetes	/	Rheumatoid
Site of infection	Left knee	Left knee	Right hip	Left knee	Left knee	Right knee	Left knee	Right knee
Since the last surgery	4 months	11months	12 months	6 years	20 days	24 months	24 months	5 months
Clinical manifestations	Sinus tract	Pain	Pain Swollen	Periprosthetic fracture	Swollen Pain Fever	Purulent exudates	Swollen Pain	Sinus tract Swollen
Duration of Symptoms	4 weeks	8 weeks	12 months	6 months	4 days	24 months	12 months	6 weeks
Initial antibiotic treatment	V	C; Flu	unclarified	V	I	/	/	/
Preoperative results (culture)	*C.glabrata*	Negative	/	*A.terreus*	*S.aureus*	Negative	Negative	Negative
Preoperative results (mNGS)	*C.glabrata*	*C.parapsilosis*	/	*A.terreus*	/	*C.pelliculosa*	*C.parapsilosis*	*C.parapsilosis*
Operative treatment	Cement spacer	Cement spacer	Cement spacer	Cement spacer	DAIR	Cement spacer	Cement spacer	/
Antimicrobial eluting cement	V 7 g; M 7 g; A 0.5 g	V 7 g; M 7 g A 0.5 g	V 6 g; M 6 g;	V 7 g; M 7 g; A 0.5 g	/	V 7 g; M 7 g; A 0.5 g	V 6 g; M 6 g A 0.5 g	/
Intraoperative result (culture)	*C.glabrata S.epidermidis*	*C.parapsilosis*	*S.epidermidis*	*A.terreus*	*S.aureus C.parapsilosis*	*C.pelliculosa*	*C.parapsilosis*	/
Intraoperative results (mNGS)	*C.glabrata S.epidermidis*	*C.parapsilosis*	*S.epidermidis A.niger*	*A.terreus*	*S.aureus C.parapsilosis*	*C.pelliculosa*	/	/
Antimicrobial treatment	Fos, Flu	Flu	V, Flu	L, Flu	I, V, Flu	Flu	Flu	Flu
Total length of antifungals	6 months	6 months	6 months	6 months	6 months	6 months	6 months	6 months
Outcome	Cured	Cured	Cured	Cured	Cured	Cured	Cured	Controlled

Abbreviations:V, vancomycin; M, meropenem; Fos; fosfomycin; A, amphotericin; C, cephalosporins ; Flu, fluconazole ; I, Imipenem ;L, levofloxacin; DAIR, debridement and implant retention.

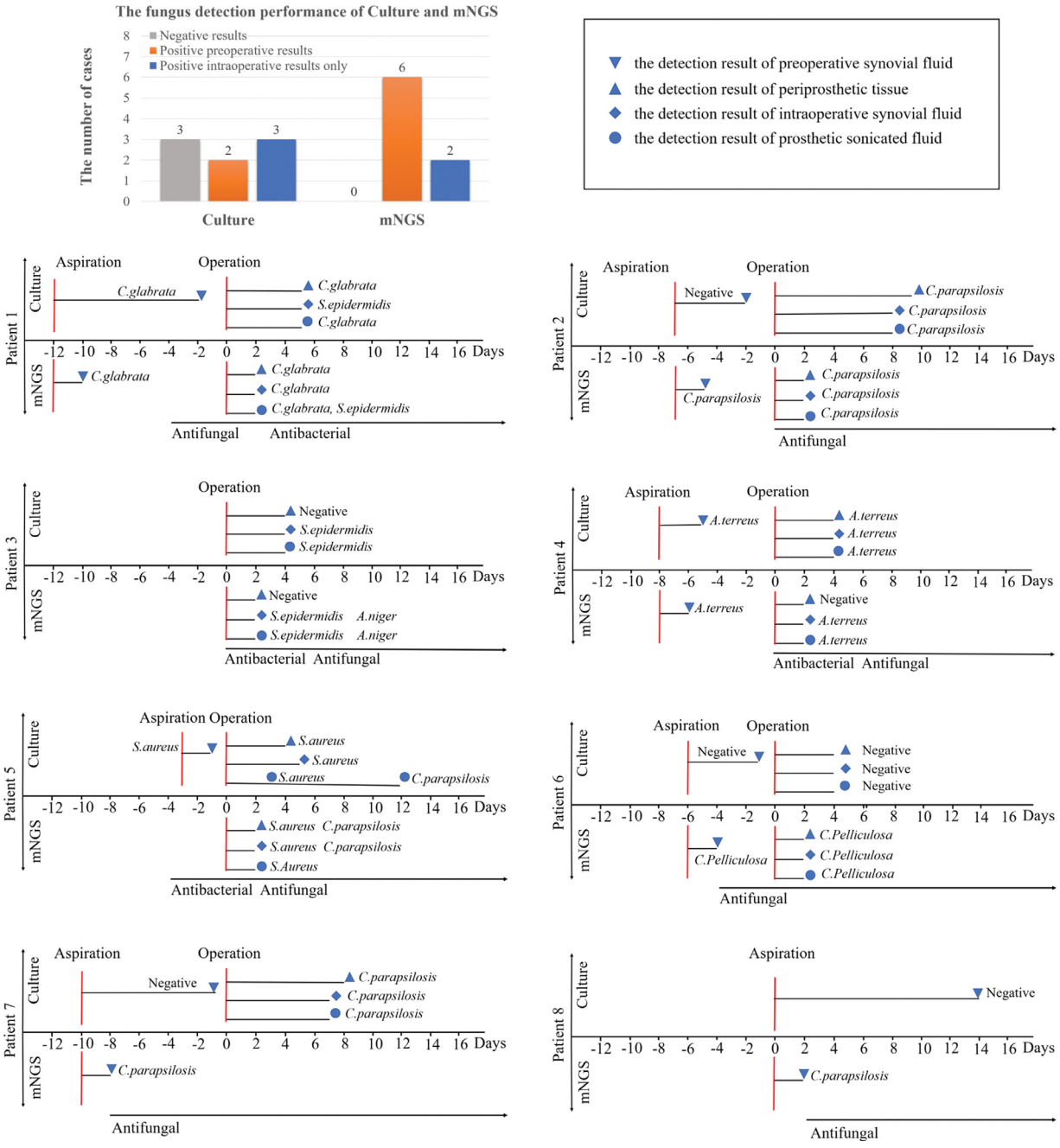

Fig. 1. The fungal detection performance of culture and mNGS for 8 patients in preoperative diagnosis and intraoperative diagnosis using four different clinical specimen types. Time and results of pathogen detection using mNGS and culture for different specimen types of each individual patient are respectively presented.

tient. After nine month's follow-up, all of the infections have been cured or controlled with the disappearance of the symptoms and serological abnormalities. mNGS played a significant role in the management of these fungal PJIs. As shown in Fig. 1, we performed mNGS detection in four clinical specimens (preoperative synovial fluid, periprosthetic tissue, intraoperative synovial fluid and prosthetic sonicated fluid) of these cases, pairing with culture of corresponding specimen. mNGS detected fungal organisms in all 8 cases, of which 6 cases were positive preoperatively and 2 cases were positive intraoperatively only. However, culture only detected fungal organisms in 5 cases, of which 2 cases were positive preoperatively and 3 cases were positive intraoperatively only. The feedback of mNGS results would be no longer than 48 h while it usually be more than 4 days for fungal culture results feedback.

For the 6 cases (including the non-operation case 8) undergoing preoperative articular aspirations for the test of both mNGS and culture, 6 cases were positive for mNGS test while only 2 cases were positive for culture. Since intraoperative infusion of bone cement with fungal drugs has been proved effectively in fungal PJI treatment, the high preoperative pathogen detection rate and the rapid detection cycle of mNGS is of great value for the surgical preparation and intraoperative medication.[6] In almost all the cases, we tested multiple samples for each case to verify the scientific value of mNGS in the pathogen diagnosis of fungal PJI. Revealed in Fig. 1, the pathogen type detected by mNGS and culture for each sample of each case is highly consistent. Therefore, we believe that

mNGS should be reliable and valuable in the pathogen detection of fungal PJI.

This is the first time in current literatures to focus on application value of mNGS in management of fungal PJIs. We could only enroll a small series of 8 patients for the present study. But for fungus PJIs rarely happened, this largest series to date are enable to figure out mNGS could effectively assist the management of fungal PJIs. Currently, the vast majority of molecular diagnostic techniques focuses on sequencing of the 16S segment, a conserved region of bacterial genome, which makes them unable to identify fungal organisms.[7,8] Untargeted mNGS shows great advantages and application value in the detection of fungal pathogens. To date, no study has indicated the definite value of mNGS in fungal PJI management. It is now well recognized.

In summary, mNGS could reliably improve the detection rate of fungal pathogens in PJIs compared with traditional culture, especially in the preoperative detection. With the progress made by mNGS, it is possible to timely select appropriate targeted antimicrobial therapy and operative treatment, further to lead to improvement of the success rate in fungal PJI treatment. Therefore, we recommend the use of mNGS as a routine workup when dealing with PJIs caused by suspected fungal pathogens.

Funding

This work was supported by the National Natural Science Foundation of China (81772364, 81772309) and Shanghai Technology Support Programs (19411962600).

Declaration of Competing Interest

The authors declare that there are no conflicts of interest.

Acknowledgments

We thank our patients for their cooperation with participating in this study. We thank the BGI Genomics, China for their great help of proceeding the mNGS test and bioinformatic analysis.

Reference

1. Zhang H.C., Ai J.W., Cui P., Zhu Y.M., Li Y.J., Zhang W.H. Incremental value of metagenomic next generation sequencing for the diagnosis of suspected focal infection in adults. *J Infect* 2019 Aug 20 PubMed PMID: 31442461. Epub 2019/08/24. eng.
2. Belden K., Cao L., Chen J., Deng T., Fu J., Guan H., et al. Hip and Knee section, fungal periprosthetic joint infection, diagnosis and treatment. *Proc Int Consensus Orthopedic Infect J Arthropl* 2019;**34**(2s):S387–Ss91 PubMed PMID: 30343967. Epub 2018/10/23. eng.
3. Pappas P.G., Kauffman C.A., Andes D.R., Clancy C.J., Marr K.A., Ostrosky-Zeichner L., et al. Clinical practice guideline for the management of candidiasis: 2016 update by the infectious diseases society of America. *Clin Infect diseas offic publ Infect Diseases Soc Am* 2016;**62**(4):e1–50 PubMed PMID: 26679628. Pubmed Central PMCID: Pmc4725385. Epub 2015/12/19. eng.
4. Simner P.J., Miller S., Carroll K.C. Understanding the promises and hurdles of metagenomic next-generation sequencing as a diagnostic tool for infectious diseases. *Clin Infect diseas offic publ Infect Diseases Soc Am* 2018 Feb 10;**66**(5):778–88 PubMed PMID: 29040428. Epub 2017/10/19. eng.
5. Dekker J.P.. Metagenomics for clinical infectious disease diagnostics steps closer to reality. *J Clin Microbiol* 2018;**56**(9) PubMed PMID: 29976592. Pubmed Central PMCID: Pmc6113477. Epub 2018/07/07. eng.
6. Kuiper J., van den Bekerom M., van der Stappen J., Nolte P., Colen S. 2-stage revision recommended for treatment of fungal hip and knee prosthetic joint infections. *Acta Orthop* 2013;**84**(6):517–23 PubMed PMID: 24171675.
7. Marín M., Garcia-Lechuz J., Alonso P., Villanueva M., Alcalá L., Gimeno M., et al. Role of universal 16S rRNA gene PCR and sequencing in diagnosis of prosthetic joint infection. *J Clin Microbiol* 2012;**50**(3):583–9 PubMed PMID: 22170934.
8. Tarabichi M., Shohat N., Goswami K., Alvand A., Silibovsky R., Belden K., et al. Diagnosis of periprosthetic joint infection: the potential of next-generation sequencing. *J Bone Joint Surgery Am Vol* 2018;**100**(2):147–54 PubMed PMID: 29342065. Epub 2018/01/18. eng.

Renke He, Qiaojie Wang, Feiyang Zhang
Department of Orthopaedics, Shanghai Jiao Tong University Affiliated Sixth People's, Hospital, Shanghai Jiao Tong University, Shanghai 200233, PR China

Jin Tang
Department of Clinical Laboratory, Shanghai Jiao Tong University Affiliated Sixth, People's Hospital, Shanghai Jiao Tong University, Shanghai 200233, PR China

Hao Shen*, Xianlong Zhang*
Department of Orthopaedics, Shanghai Jiao Tong University Affiliated Sixth People's, Hospital, Shanghai Jiao Tong University, Shanghai 200233, PR China

*Corresponding authors.
E-mail addresses: shenhao7212@sina.com (H. Shen), dr_zhangxianlong@163.com (X. Zhang)

Accepted 11 September 2020
Available online 19 September 2020

https://doi.org/10.1016/j.jinf.2020.09.013

© 2020 The British Infection Association. Published by Elsevier Ltd. All rights reserved.

Genetic characterization of a novel genotype H9N2 avian influenza virus from chicken in South China

Dear Editor,

Recently, the emergence of a novel reassortant H7N2 avian influenza virus (AIV) was reported in this journal, and the genetic characteristics suggested this novel H7N2 AIV was a reassortant virus of H7N9 and H9N2 AIVs that are circulating in China.[1] H9N2 AIV binds to both human and avian receptors efficiently and has caused occasionally human infections in Asia[2]. Meanwhile, the H9N2 AIV continued to act as genetic donor to multiple novel AIVs, including H7N9, H10N8, H6N1, H6N2, and H5N1.[3] The novel H7N2 showed distinct antigenicity to the vaccine seed strain, which suggested the importance of continuing surveillance of the prevalence of H7N9 and H9N2 strains. In this study, we report a novel genotype ressortant H9N2 strain, A/chicken/Baise/0701/2019(H9N2) (BS/2019), isolated from an acutely ill chicken farm in Baise city, China during the routine surveillance.

The virus was grown in embryonated chicken eggs for 48 h at 37 °C, and RNA was extracted using a viral DNA/RNA miniprep Kit (Axygen, China). The reverse transcription was subsequently performed using the ProtoScript II First Stand cDNA Synthesis Kit (NEB, USA). The full lengths of all eight viral segments were amplified using a set of universal primers as described by Hoffmann et al.[4] with a Q5 high -fidelity master mix (NEB, USA), and subcloned into the pMD-18T vector for sequencing(Sangon Biotech, China). The 100% of the coding regions of all segments were obtained with the $G+C$ content from 41.18% to 41.87%. The hemagglutinin (HA) proteolytic cleavage site of BS/2019 was PSRSSR/GLF, which is a characteristic of low pathogenic AIVs[5]. The mammalian host-specific residue L226 (H3 numbering) was found at the receptor binding site of HA protein, suggesting that the virus preferentially binds human-like receptors[6]. Meanwhile, the residues R207K and H436Y in PB1 protein and A515T in PA protein that have been shown to increase the polymerase activity in mammalian cells were found in BS/2019. Mammalian host specific markers, includ-

ing V15I andN30D, were found in the M1 protein. However, the PB2 protein had E627and D701 residues, and the NP protein had an AIV biomarker E372, suggesting this virus are not yet fully adapted to mammals.[7] The virulence-related biomarkers M677T in the PB1 protein and P42S and F103L in the NS1 protein were found in the PB1 protein, which suggested increased virulence of H9N2 AIVs in the mammalian hosts.

The nucleotide sequences of all eight gene segments in BS/2019 were aligned by ClustalW and phylogenetically clustered by MEGA7 as previously described.[8] The maximum likelihood trees were constructed based on the Tamura-Nei model. and the evolutionary distances were estimated between two sequences. Our phylogenic analysis revealed the HA genes of BS/2019 belonged to the group Y280 of the Eurasian lineage (Fig. 1A). However, the homological analysis results showed the BS/2019 and A/Duck/Hong Kong/Y280/97 only shared 87.5% similarity at the nucleotide level and 88.7% similarity at the amino acid level. Homology blast showed the HA sequence was most closely related to the H9N2 virus isolated from south Vietnam and south China (A/chicken/Vietnam/HU9–506/2018(H9N2)), with the identity of 98.75%. Of note, the HA of BS/10 showed high identity to two H9N2 human isolates in recent years (Fig. 1A). Neuraminidase (NA) nucleotide sequences belonged to the group Y280 and had a high identity (98.43%) to H9N2 virus isolated from eastern China since 2015 (Fig. 1B).

The internal genes, PB1, PA, NP, and NS were in close proximity to the F98 lineage viruses. In contrast, the PB2 and M belonged to the G1 lineage and had the highest identity to the chicken H9N2 virus isolated from Vietnam. Based on these findings, we suggested that the new genotype BS/2019 was a reassortant between G1, Y280, and F98 lineage viruses. N-linked glycosylation (abbreviates G) of HA and NA, which add oligosaccharides to Asn-residue by N-glycosidic linkages, plays an important role in multiple biological activities of AIVs. BS/19 had 8 (29G$^+$, 82 G^+, 141 G^+, 298 G^+, 305 G^+, 313 G^+, 492 G^+, and 551 G^+) and 6 (66 G^+, 83 G^+,143 G^+,197 G^+, 231G$^+$, and 365 G^+) N-linked glycosylation sites on HA (Fig. 1C) and NA (Fig. 1D), respectively, according to the consensus N-X-S/T (X can be any amino acid except proline) glycosylation motif. In contrast, the phenotype of Y280 was 218G$^+$/313G$^-$/551G$^-$.

Our results suggested there are variations in the glycosylation sites at the residues 218, 313, and 551 during the evolution of H9N2 IAVs. The BS/19 lost a glycosylation site at residue 44 of NA. Remarkably, glycosylation at the residue 44 of NA was absent in the 1918 and 2009 pandemic virus and was suggested as a pandemic associated signature[9]. The 44 G shift in the glycosylation site of NA could serve as a potential characteristic of the pandemic.

We further propagated the BS/19 in SPF chicken embryo eggs for 48 h, and the HA titers reached 128HAU/50 μl by the HA assay with 0.5% chicken red blood cells. We further determined the antigenicity of BS/19 by the hemagglutination inhibition (HI) test using a panel of 5 reference sera from vaccinated chicken farms as previously described.[10] The HI titer of BS/19 had a 2.8 ± 1.09-fold change compared to that of the standard H9 antigen. Our results suggested a poor antigenic match between the vaccine strain and the circulating strains. Robust genotype monitor and laboratory surveillance are required for H9N2 IAV.

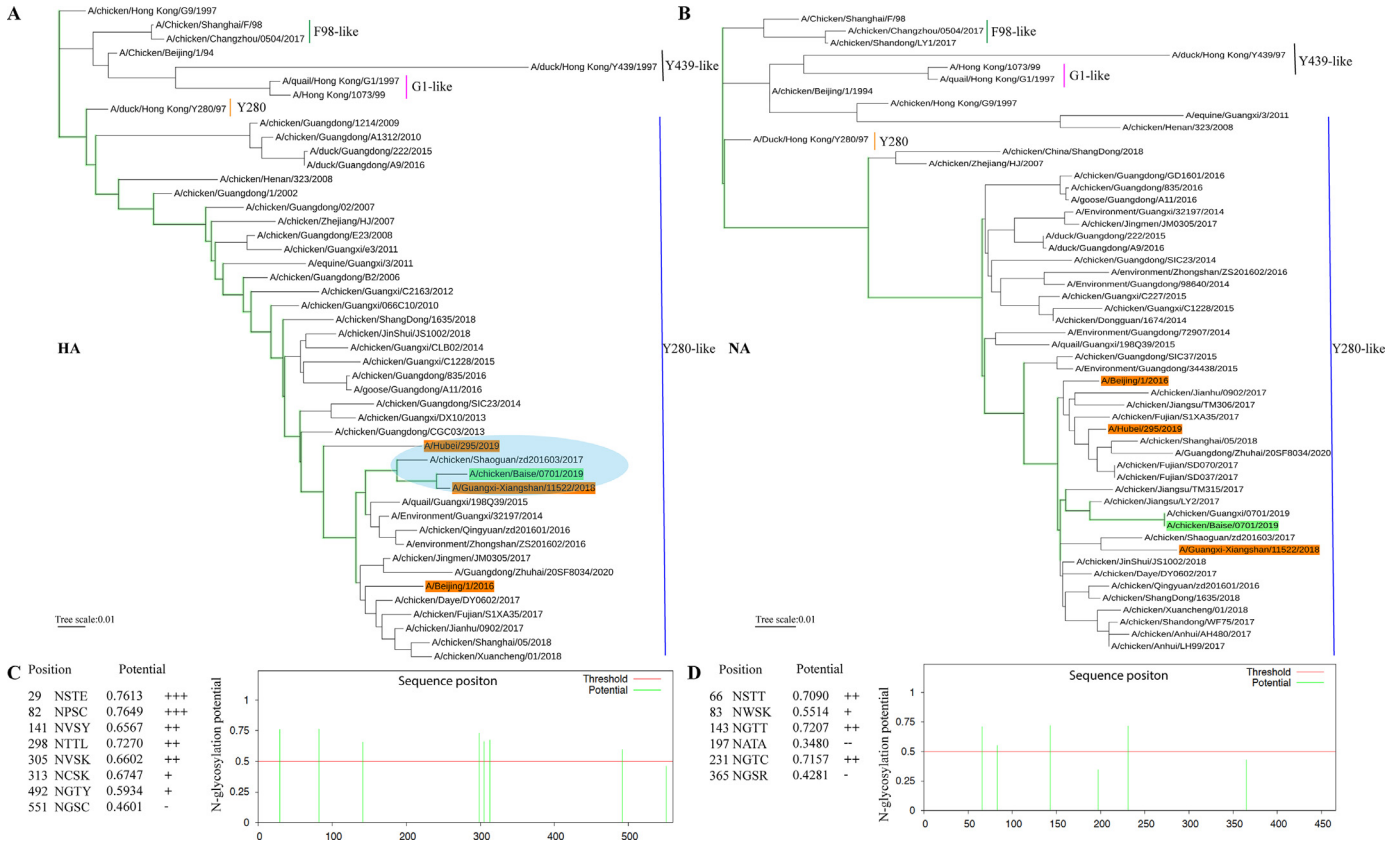

Fig. 1. Phylogenetic and glycosylation analyses of the HA and NA gene sequences from recent H9N2 isolates. The reference sequences were extracted from the GenBank and GISAID. Phylogenetic trees were constructed by MEGA7. Sequences with orange background represents human isolates. (A) Phylogenetic tree of HA gene for H9N2 AIV. The oval in Light Blue highlights the H9N2 AIV close to the human isolates. (B) Phylogenetic tree of NA gene for H9N2 IAV. (C) Glycosylation analyses of the HA gene for H9N2 IAV. (D) Glycosylation analyses of the NA gene for H9N2 IAV. Glycosylation sites were predicted by the consensus N-X-S/T glycosylation motif. The potential of the glycosylation sites was calculated by the NetNGlyc 1.0 Server(http://www.cbs.dtu.dk/services/NetNGlyc/).

Funding information

This study was supported by National Natural Science Foundation of China (Grant No. 32002320); Natural Science Foundation of Guangdong Province, China (Grant No. 2020A1515010116); Medical Scientific Research Foundation of Guangdong Province, China (Grant No. A2020083); Modern agricultural industry technology system innovation team of Guangdong Province (Grant No. 2019KJ137); National Key Research and Development Project (Grant No. 2017YFD0500800).

Declaration of Competing Interest

All authors declare no conflict of interest.

Reference

1. Qiu Y., Sun R., Hou G., Yu X., Li Y., Li J., et al. Novel reassortant H7N2 originating from the H7N9 highly pathogenic avian influenza viruses in China. *J Infect* 2019;**79**(5):462–70 PubMed PMID: 31473272. Epub 2019/09/02.
2. Pan Y., Cui S., Sun Y., Zhang X., Ma C., Shi W., et al. Human infection with H9N2 avian influenza in northern China. *Clin Microbiol Infect* 2018;**24**(3):321–3 PubMed PMID: 29104171. Epub 2017/11/07.
3. Liu D., Shi W., Gao G.F. Poultry carrying H9N2 act as incubators for novel human avian influenza viruses. *Lancet* 2014;**383**(9920):869 PubMed PMID: 24581684. Epub 2014/03/04.
4. Hoffmann E., Stech J., Guan Y., Webster R.G., Perez D.R. Universal primer set for the full-length amplification of all influenza a viruses. *Arch Virol* 2001;**146**(12):2275–89 PubMed PMID: 11811679. Epub 2002/01/29.
5. Guo Y.J., Krauss S., Senne D.A., Mo I.P., Lo K.S., Xiong X.P., et al. Characterization of the pathogenicity of members of the newly established H9N2 influenza virus lineages in Asia. *Virology* 2000;**267**(2):279–88 PubMed PMID: 10662623. Epub 2000/02/09.
6. Wan H., Sorrell E.M., Song H., Hossain M.J., Ramirez-Nieto G., Monne I., et al. Replication and transmission of H9N2 influenza viruses in ferrets: evaluation of pandemic potential. *PLoS ONE* 2008;**3**(8):e2923 PubMed PMID: 18698430. Pubmed Central PMCID: PMC2500216. Epub 2008/08/14.
7. Bi Y., Zhang Z., Liu W., Yin Y., Hong J., Li X., et al. Highly pathogenic avian influenza A(H5N1) virus struck migratory birds in China in 2015. *Sci Rep* 2015;**5**:12986 PubMed PMID: 26259704. Pubmed Central PMCID: PMC4531313. Epub 2015/08/12.
8. Guo J., Huang S., Wen F. Identification of coevolution sites and evolution history for neuraminidase of human influenza A viruses. *J Infect* 2020;**80**(2):232–54 PubMed PMID: 31634491. Epub 2019/10/22.
9. Kim P., Jang Y.H., Kwon S.B., Lee C.M., Han G., Seong B.L. Glycosylation of hemagglutinin and neuraminidase of influenza a virus as signature for ecological spillover and adaptation among influenza reservoirs. *Viruses* 2018;**10**(4) PubMed PMID: 29642453. Pubmed Central PMCID: PMC5923477. Epub 2018/04/13.
10. Wen F., Li L., Zhao N., Chiang M.J., Xie H., Cooley J., et al. A Y161F hemagglutinin substitution increases thermostability and improves yields of 2009 h1n1 influenza a virus in cells. *J Virol* 2018;**92**(2) PubMed PMID: 29118117. Pubmed Central PMCID: PMC5752953. Epub 2017/11/10.

Feng Wen, Wenfeng Li, Jinyue Guo, Jing Yang, Xuelian Zhang, Kun Mei, Hao Liu, Saeed El-Ashram
College of Life Science and Engineering, Foshan University, No. 33 guangyun road, Shishan town, Nanhai district, Foshan 528231, Guangdong, China

Kaijian Luo
College of Veterinary Medicine, South China Agricultural University, Guangzhou 510642, Guangdong, China

Sheng Yuan*, Shihong Chi*, Shujian Huang*
College of Life Science and Engineering, Foshan University, No. 33 guangyun road, Shishan town, Nanhai district, Foshan 528231, Guangdong, China

*Corresponding authors
E-mail addresses: fsyuans@126.com (S. Yuan), chishihong@fosu.edu.cn (S. Chi), huangshujian@fosu.edu.cn (S. Huang)

Accepted 3 September 2020
Available online 19 September 2020

https://doi.org/10.1016/j.jinf.2020.09.011

© 2020 The British Infection Association. Published by Elsevier Ltd. All rights reserved.

Horizontal transfer of *bla*$_{NDM-1}$-carrying IncX3 plasmid between carbapenem-resistant *Enterobacteriaceae* in a single patient

Dear Editor,

Carbapenems represent the most potent treatment option for severe infections caused by gram-negative bacteria. Recently, a rapid increase in carbapenem-resistant *Enterobacteriaceae* (CRE) has led to therapeutic challenges and has become an ongoing serious public health concern.[1] Carbapenemases can hydrolyze the carbapenems and most of the beta-lactam antibiotics;[2] they are mainly located on a variety of plasmids, which can be transferred to other bacteria.[3] There are a few known plasmids capable of horizontally transmitting of carbapenemase genes to other *Enterobacteriaceae*, including incompatibility groups of IncX3 responsible for the dissemination of a carbapenemase gene *bla*$_{NDM}$.[4] Several studies have reported interspecies and intraspecies transfer of carbapenemase genes in a single patient.[3,5,6] However, obtaining direct evidence for *in vivo* transfer can be challenging because it is difficult to designate the original recipient strain that later gained a new resistant gene from a donor strain. Here, based on comparative genomic analysis, we describe the horizontal transfer of *bla*$_{NDM-1}$-carrying IncX3 plasmid by identifying both potential donor and recipient strains isolated from a patient.

In February 2018, a 73-year-old female patient with a history of cerebrovascular accident was transferred from a general hospital to a nursing hospital for the elderly. During the hospital stay, stool samples were taken and screened for CRE as a part of infection control. Bacterial identification was performed using VITEK 2 (bioMérieux, Marcy l'Etoile, France). Antimicrobial susceptibility testing was performed using a broth microdilution method (TREK Diagnostic Systems, Cleveland, USA), and the minimum inhibitory concentrations (MICs) were interpreted in accordance with Clinical & Laboratory Standards Institute (CLSI) guidelines. PCR and sequencing were used to identify the carbapenemase genes.[7] Pulsed-field gel electrophoresis (PFGE) was carried out according to standardized PulseNet protocols (http://www.pulsenetinternational.org). Conjugation was performed with broth mating using azide-resistant *Escherichia coli* J53 as a recipient strain. Plasmid incompatibility groups were assigned with PCR-based replicon typing,[8] and plasmid contents and sizes were estimated using S1 nuclease-treated PFGE. No ethical approval was needed for this study; the isolates used were collected as a part of routine diagnosis in a clinical setting, and the data were anonymously analyzed.

In September, a *bla*$_{KPC-2}$-harboring *Klebsiella aerogenes* strain SECR18-1644 was isolated from the patient, and then, an additional carbapenemase gene *bla*$_{NDM-1}$ was detected in the *K. aerogenes* strain (SECR18-2341) isolated in November. Both isolates were resistant against penicillins, cephems and carbapenems, but strain SECR18-2341 was highly resistant to third-generation cephalosporins, as usually observed for NDM producers (Table 1). By multi-locus sequence typing analysis (https://pubmlst.org/kaerogenes/), it was confirmed that they belonged to the sequence type 202 (ST202), and exhibited nearly identical *Xba*I-PFGE patterns (96.8% similarity; Supplementary Figure S1), suggesting

Table 1
Characteristics of carbapenem-resistant isolates and their transconjugants.

Isolates	Isolation date	Species	Carbapenemases	Inc types	MIC (mg/L)*									
					AMP	CTX	TET	GEN	SXT	CIP	CHL	IMI	MER	ERT
SECR18-1551	2018.09.	*Citrobacter freundii*	bla_{NDM-1}	X3	>64	>64	≤2	≤1	≤1	2	4	4	8	8
SECR18-1644	2018.09.	*Klebsiella aerogenes*	bla_{KPC-2}	FII_K	>64	16	4	≤1	≤1	≤0.03	8	4	2	4
SECR18-2341	2018.11.	*Klebsiella aerogenes*	bla_{KPC-2}, bla_{NDM-1}	FII_K, X3	>64	>64	4	≤1	≤1	≤0.03	8	8	4	8
Transconjugants														
18-1551-TC-N		*Escherichia coli, J53*	bla_{NDM-1}	X3	>64	64	≤2	≤1	≤1	≤0.03	8	4	≤0.5	4
18-1644-TC-K		*Escherichia coli, J53*	bla_{KPC-2}	FII_K	>64	8	≤2	≤1	≤1	≤0.03	8	1	≤0.5	1
18-2341-TC-N		*Escherichia coli, J53*	bla_{NDM-1}	X3	>64	>64	≤2	≤1	≤1	≤0.03	8	4	≤0.5	2
18-2341-TC-K		*Escherichia coli, J53*	bla_{KPC-2}	FII_K	>64	16	≤2	≤1	≤1	≤0.03	8	2	1	1
J53 (recipient)		*Escherichia coli, J53*			4	≤1	≤2	≤1	≤1	≤0.03	4	≤0.5	≤0.5	≤0.25

*AMP, ampicillin; CTX cefotaxime; TET, tetracycline; GEN, gentamicin; SXT, trimethoprim-sulfamethoxazole; CIP, ciprofloxacin; CHL, chloramphenicol; IMI, imipenem; MER, meropenem; ERT, ertapenem.

that the bla_{KPC-2}-positive *K. aerogenes* may have acquired the second carbapenemase gene bla_{NDM-1}.

Given that *Citrobacter freundii* strain carrying bla_{NDM-1} (SECR18-1551) was also isolated in September from the same patient, we hypothesized that bla_{NDM-1} in SECR18-2341 may have been originated from SECR18-1551. The bla_{NDM-1} genes in two isolates were successfully transferred to *E. coli* J53 by conjugation. S1-PFGE and replicon typing showed that both strains and their transconjugants harbored an ~45 kb IncX3 plasmid, which was not detected in SECR18-1644 that did not carry the bla_{NDM-1} (Supplementary Figure S2). These results demonstrated that bla_{NDM-1} in *C. freundii* (SECR18-1551) and *K. aerogenes* (SECR18-2341) was likely located on the same IncX3 plasmid.

Whole genome sequencing of SECR18-2341 was performed using PacBio RSII (Pacific Biosciences, Menlo Park, USA) combined with Illumina HiSeq (San Diego, CA, USA). Sequence reads were *de novo* assembled using the hierarchical genome-assembly process and polished with Pilon v1.21. Plasmids of SECR18-1551 and SECR18-1644 were sequenced using HiSeq and assembled with SPAdes v3.11.1. The genome was annotated using the NCBI

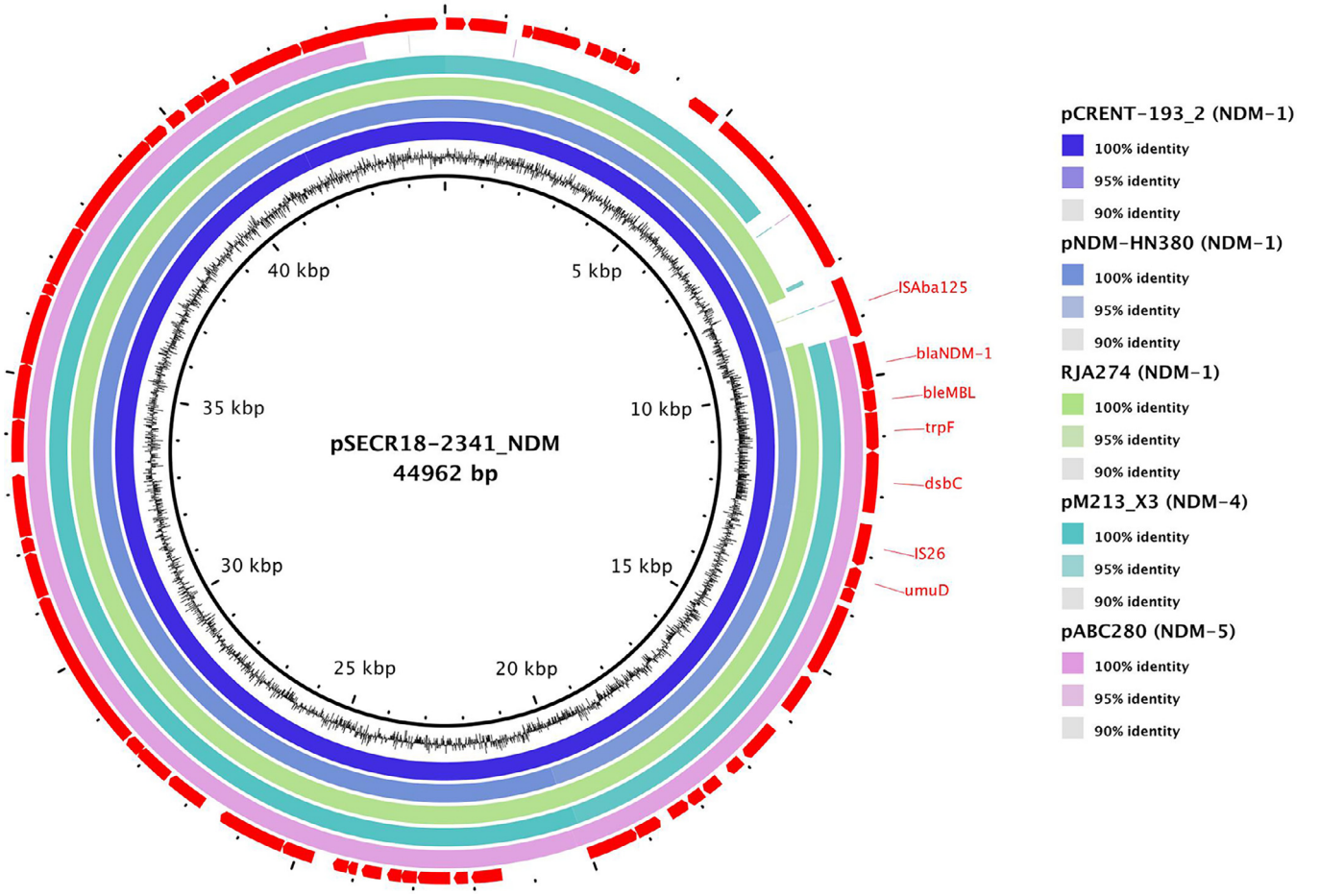

Figure 1. Alignment of bla_{NDM}-carrying IncX3 plasmids. The nucleotide sequences pSECR18-2341_NDM in *Klebsiella aerogenes* strain SECR18-2341 and five closely related plasmids, pCRENT-193_2 in *Enterobacter* spp. (GenBank accession no. **CP024814**), pNDM-HN380 in *K. pneumoniae* (GenBank accession no. **JX104760**), RJA274 plasmid NDM-1 in *Raoultella planticola* (GenBank accession no. **KF877335**), pM213_X3 in *Escherichia coli* (GenBank accession no. **AP018142**) and pABC280-NDM-5 in *E. coli* (GenBank accession no. **MK372392**) were compared using BLAST Ring Image Generator.

Prokaryotic Genomes Annotation Pipeline and analyzed using ResFinder (https://cge.cbs.dtu.dk/services/ResFinder/). Nucleotide sequences were deposited at GenBank under the accession numbers **CP049600-CP049602** and **MT129534-MT129535**.

The strain SECR18-2341 has a single circular chromosome of 5,241,093 bp containing 4,960 predicted protein-coding sequences and two distinct plasmids, named pSECR18-2341_NDM and pSECR18-2341_KPC. No antimicrobial resistance determinants were found except for two carbapenemase genes, consistent with the phenotypic resistance profile. The bla_{NDM-1}-containing plasmid pSECR18-2341_NDM was 44,962 bp and carried 57 proteins with a conserved plasmid backbone responsible for conjugal transfer and replication. This plasmid, including the genetic content (IS*Aba125*-bla_{NDM-1}-ble_{MBL}-*trpF-dsbC*-IS*26-umuD*), showed a perfect match with a previously described bla_{NDM-1}-carrying IncX3 plasmid in *Enterobacter* (pCRENT-193_2; GenBank accession no. **CP024814**) isolated in Korea in 2013 (Figure 1). Based on sequence data, the bla_{NDM-1}-carrying IncX3 plasmids in SECR18-2341 (pSECR18-2341_NDM) and SECR18-1551 (pSECR18-1551_NDM) were identical, strongly supporting the hypothesis of lateral transfer of plasmid-borne bla_{NDM-1} between the different species—*C. freundii* (SECR18-1551; the potential donor) and *K. aerogenes* (SECR18-1644; the potential recipient)—resulting in the emergence of *K. aerogenes* SECR18-2341 carrying both bla_{NDM-1} and bla_{KPC-2} genes.

The plasmid carrying bla_{KPC-2} (pSECR18-2341_KPC) was an $IncFII_K$ plasmid of 119,990 bp, which was closely related to the bla_{KPC-2}-encoding plasmid pJYC01A in *K. pneumoniae* (GenBank accession no. **CP022926**), the *Klebsiella pneumoniae* carbapenemase (KPC) outbreak strain in Korea, 2014. The bla_{KPC-2} was flanked by the insertion sequences IS*Kpn7* and IS*Kpn6* embedded within a Tn*3*-based Tn*4401* transposon. Two bla_{KPC-2}-carrying plasmids in both *K. aerogenes* SECR18-1644 and SECR18-2341 were highly similar, with the exception of an 8.1-kb duplication of IS*Kpn25* in pSECR18-2341_KPC (Supplementary Figures S2 and S3).

Long-term hospitalization of patients is a risk factor for the acquisition and subsequent transmission of new antimicrobial resistance traits. Patients can be more vulnerable to infection with resistant bacteria, because of their susceptible medical conditions and relatively high levels of contamination in residential environments. Moreover, persistent gastrointestinal carriage of resistant bacteria in such patients can contribute to the resistant gene dispersion between co-colonizing strains.[9,10] Recent studies have reported that IncX3 plasmids showed efficient horizontal mobility for various recipient sources and over ambient temperatures,[11] serving as important vehicles for the global spread of carbapenemase genes.[4] In conclusion, we found evidence of *in vivo* horizontal transfer of IncX3 plasmid carrying bla_{NDM-1} between *Enterobacteriaceae* occupying the same ecological niche in a single patient. Multiple acquisitions and dissemination of various resistance genes via self-transferrable plasmids may contribute to the development of multidrug resistance, thus posing complications in treating infections caused by these strains.

Declarations of Competing interest

The authors declare no conflict of interest.

Funding

This research did not receive any specific grant from funding agencies in the public, commercial, or not-for-profit sectors.

Supplementary materials

Supplementary material associated with this article can be found, in the online version, at doi:10.1016/j.jinf.2020.07.013.

References

1. Tran DM, Larsson M, Olson L, Hoang NTB, Le NK, Khu DTK, et al. High prevalence of colonisation with carbapenem-resistant *Enterobacteriaceae* among patients admitted to Vietnamese hospitals: Risk factors and burden of disease. *J Infect* 2019;**79**:115–22.
2. Queenan AM, Bush K. Carbapenemases: the versatile beta-lactamases. *Clin Microbiol Rev* 2007;**20**:440–58.
3. Sidjabat HE, Silveira FP, Potoski BA, Abu-Elmagd KM, Adams-Haduch JM, Paterson DL, et al. Interspecies spread of *Klebsiella pneumoniae* carbapenemase gene in a single patient. *Clin Infect Dis* 2009;**49**:1736–8.
4. Ho PL, Li Z, Lo WU, Cheung YY, Lin CH, Sham PC, et al. Identification and characterization of a novel incompatibility group X3 plasmid carrying bla_{NDM-1} in *Enterobacteriaceae* isolates with epidemiological links to multiple geographical areas in China. *Emerg Microbes Infect* 2012;**1**:e39.
5. Goren MG, Carmeli Y, Schwaber MJ, Chmelnitsky I, Schechner V, Navon-Venezia S. Transfer of carbapenem-resistant plasmid from *Klebsiella pneumoniae* ST258 to *Escherichia coli* in patient. *Emerg Infect Dis* 2010;**16**:1014–17.
6. Gottig S, Gruber TM, Stecher B, Wichelhaus TA, Kempf VA. In vivo horizontal gene transfer of the carbapenemase OXA-48 during a nosocomial outbreak. *Clin Infect Dis* 2015;**60**:1808–15.
7. Yoon EJ, Kang DY, Yang JW, Kim D, Lee H, Lee KJ, et al. New Delhi Metallo–beta-lactamase-producing *Enterobacteriaceae* in South Korea between 2010 and 2015. *Front Microbiol* 2018;**9**:571.
8. Carattoli A, Bertini A, Villa L, Falbo V, Hopkins KL, Threlfall EJ. Identification of plasmids by PCR-based replicon typing. *J Microbiol Methods* 2005;**63**:219–28.
9. Drieux L, Bourgeois-Nicolaos N, Cremniter J, Lawrence C, Jarlier V, Doucet-Populaire F, et al. Accumulation of carbapenemase-producing Gram-negative bacteria in a single patient linked to the acquisition of multiple carbapenemase producers and to the *in vivo* transfer of a plasmid encoding VIM-1. *Int J Antimicrob Agents* 2011;**38**:179–80.
10. McInnes RS, McCallum GE, Lamberte LE, van Schaik W. Horizontal transfer of antibiotic resistance genes in the human gut microbiome. *Curr Opin Microbiol* 2020;**53**:35–43.
11. LeWang Y, Tong MK, Chow KH, Cheng VC, Tse CW, Wu AK, et al. Occurrence of highly conjugative IncX3 epidemic plasmid carrying bla_{NDM} in *Enterobacteriaceae* isolates in geographically widespread areas. *Front Microbiol* 2018;**9**:2272.

Jin Seok Kim, Young-hee Jin, Sang-Hun Park, Sunghee Han, Hee Soon Kim, Jin Kyung Yu, Jung Im Jang
Infectious Diseases Team, Seoul Metropolitan Government Research Institute of Public Health and Environment, Gyeonggi-do, Republic of Korea

Junyoung Kim
Division of Bacterial Diseases, Korea Centers for Diseases Control & Prevention, Chungcheongbuk-do, Republic of Korea

Chae-Kyu Hong, Jib-Ho Lee, Sang-Me Lee, Young-Hee Oh
Infectious Diseases Team, Seoul Metropolitan Government Research Institute of Public Health and Environment, Gyeonggi-do, Republic of Korea

*Corresponding author. Tel: +82-2-570-3340; Fax: +82-2-570-3418
E-mail address: babygogs@seoul.go.kr (J.S. Kim)

Accepted 9 July 2020
Available online 13 July 2020

https://doi.org/10.1016/j.jinf.2020.07.013

© 2020 The British Infection Association. Published by Elsevier Ltd. All rights reserved.

Treatment of giardiasis in children: Randomized trial of rectal metronidazole versus oral tinidazole

Dear Editor,

Zimmermann and colleagues, in this Journal, drew attention to potential changes in healthy microbiota caused by ingested antibiotics.[1] We conducted a clinical trial to evaluate the efficacy and safety of rectal metronidazole in the treatment of *Giardia duodenalis* (*G.duodenalis*) infection in children.

A protozoan *G.duodenalis* infects small intestine of humans with the incubation period of 7–28 days. Infection can remain asymptomatic or present as diarrhea, abdominal pain or failure to thrive. In Nordic countries, including Finland, prevalence of giardiasis is 5.8% in symptomatic population.[2] A single positive stool enzyme immunoassay for *G.duodenalis* antigen provides a diagnostic sensitivity close to 100% and specificity of > 90%.[3] Nitroimidazoles represent the drugs of choice for giardiasis, particularly single-dose oral tinidazole.[4] Side effects of nitroimidazoles are usually mild and self-limited, including abdominal pain, nausea, diarrhea, metallic/bitter taste, headache and dizziness.[4] However, oral administration of nitroimidazoles in children often proves difficult in the absence of palatable pediatric formulations. Rectal tinidazole had been historically used for giardiasis treatment in Finland until the drug became unavailable. Rectal metronidazole has demonstrated efficacy in the treatment of vaginal trichomoniasis[5] and in the prophylaxis of postoperative wound infections.[6,7] Rectal administration of metronidazole results in lower serum concentrations, necessitating higher dosage.[8,9]

This open-label trial (ClinicalTrials.gov Identifier: NCT02942485, registered on 24th of October 2016) was conducted at the Children's Hospital, Helsinki University Hospital from 1.1.2017 to 1.11.2019. The study protocol was approved by the Institutional Ethic's Board (HUS/1065/2016) and by the Finnish Medicines Agency (FIMEA, KLnro 145/2016, EudraCT 2016-001938-96). The study was conducted in accordance with the Declaration of Helsinki and national and institutional standards. Informed consent was obtained from the caregivers and from patients aged ≥ 7 years.

The Epidemiologic Operations Unit of the City of Helsinki (600,000 inhabitants) yearly advertised the possibility to refer a child with giardiasis to the Children's Hospital for treatment. The authors then recruited the referred children whose clinical symptoms were compatible with giardiasis and whose stool samples tested positive for *G.duodenalis* in HUSLAB laboratory. Exclusion criteria were: 1) age < 6 months or > 10 years, 2) weight < 9.5 kg, 3) the absence of symptoms, and 4) co-infection with another intestinal pathogen. We assessed clinical response to treatment, side effects and parental acceptance of the formulation during interviews with patients/caregivers at primary visits and by phone at the follow-up.

We randomized patients at primary visits alternately into two groups by random allocation. Group 1 was treated with oral tinidazole (Fasigyn®) at a single dose of 50 mg/kg, maximum 2 g/dose. Group 2 was given rectal metronidazole (Flagyl®) for three consecutive days at 500/1000/1500 mg/dose/day for children weighing 10–14.9/15–29.9/30–44.9 kg, respectively. The doses of rectal metronidazole were arbitrary derived from the maximum oral dose (two grams) in adults. The first dose of metronidazole was administered by research nurse and two subsequent doses by caregivers at home. Clinical cure was defined as the resolution of symptoms by day 10 post-treatment. Stool samples for enzyme immunoassay were collected on day 7–10 post-treatment. If patients did not clear the infection, Group 1 was re-treated by rectal metronidazole and Group 2 by oral tinidazole (cross-over). We did not measure metronidazole serum concentrations.

The study was terminated due to the extremely slow patient enrollment: eight patients only have been referred and recruited during the two-year period (Fig. 1). This may reflect the low prevalence of giardiasis in the City of Helsinki, the inefficient advertising, or the unwillingness of primary care practitioners to refer children with an easily treatable condition. At the final stage of data analysis we discovered that 6/8 patients fulfilled one or more of the exclusion criteria. Four children were asymptomatic, and *G.duodenalis* was detected during their routine immigrant evaluation. Five patients were co-infected with other pathogens (*Shigella spp* and *Campylobacter jejuni* ($n = 1$), *Hy-*

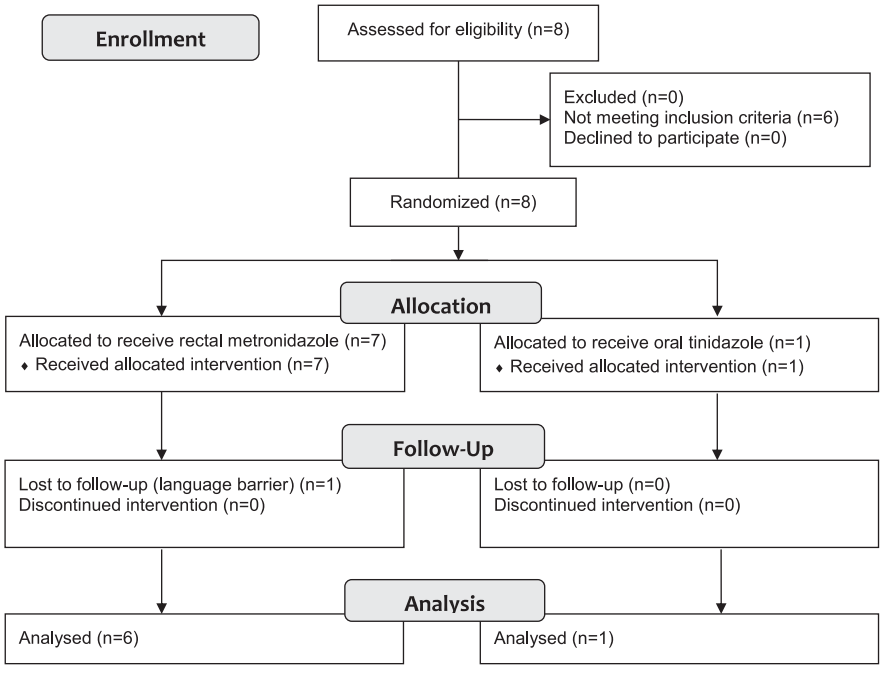

Fig. 1. Flow diagram of the patient enrollment.

Table 1
Summary of the clinical trial of rectal metronidazole compared with oral tinidazole in children with *Giardia duodenalis* infection.

Patient	Age group at recruitment, years	Symptoms compatible with giardiasis	Treatment group	Clinical cure	Microbiological eradication	Side effects
1	1–3	abdominal pain, flatulence	rectal metronidazole	yes	yes	no
2	1–3	abdominal pain, flatulence, intermittent diarrhea	rectal metronidazole	yes	yes	loose stool once after the third dose
3	1–3	abdominal pain, diarrhea, flatulence, weight loss	rectal metronidazole	yes	n/a	no
4	1–3	none	rectal metronidazole	n/a	yes	no
5	5–8	none	rectal metronidazole	n/a	yes	no
6	1–3	intermittent diarrhea	rectal metronidazole	yes	yes	no
7	5–8	none	oral tinidazole	n/a	yes	no

n/a not applicable.

menolepis nana ($n=1$), *Dientamoeba fragilis* ($n=1$) and *Blastocystis hominis* ($n=4$)). One asymptomatic patient was excluded from further analysis due to incomplete follow-up (language barrier). Thus, we next describe outcomes for six patients treated with rectal metronidazole and one patient treated with oral tinidazole (Table 1).

Median age of the patients at recruitment was 2.6 years (range 1.8–6.7 years). None had chronic illnesses or regular medications. All participants completed treatment without interruptions. Microbiological eradication was successful after the first treatment course in 6/6 tested patients (five treated with rectal metronidazole and one with oral tinidazole). All four symptomatic patients were clinically cured with rectal metronidazole. For one of them (Patient 3), the follow-up stool sample was unavailable. This patient's diarrhea recurred seven weeks post-treatment, and *G.duodenalis* was again detected in stool sample, indicating either treatment failure or re-infection. The patient received oral tinidazole with no response. After treatment with mepacrine hydrochloride according to the institutional guidelines, *G.duodenalis* was eradicated and the child was clinically cured.

Side effects were reported in one patient as a single episode of loose stool after the third dose of rectal metronidazole. The caregivers were asked to rate the ease of administration of rectal metronidazole at home, according to the suggested scale (very difficult/difficult ($n=1$) / relatively easy ($n=4$) / easy / very easy ($n=1$)). All caregivers in the rectal metronidazole group, but not the caregiver of a child who had received oral tinidazole, would opt for the same treatment modality in future. These results demonstrate the high rate of acceptability of rectal metronidazole by caregivers.

In conclusion, this is the first study evaluating the efficacy and safety of rectal metronidazole in children with giardiasis. We carefully planned the open-labeled randomized comparison study, which was, however, unsuccessful due to the insufficient recruitment rate. Therefore, our results are observational and call for further larger trials. Despite the small sample size, and thus the descriptive nature of the trial, this study provides encouraging preliminary data. We demonstrated clinical cure and microbiological eradication in 4/4 and 5/5 patients with giardiasis, respectively, after a three-day course of rectally administered metronidazole. Our study provides proof-of-concept for rectal use of metronidazole in pediatric giardiasis.

Funding

This research did not receive any specific grant from funding agencies in the public, commercial, or not-for-profit sectors. All medicines for the study were covered by the Hospital for Children and Adolescents, Helsinki University Hospital as a part of routine patient care.

Author contribution

ES and SV designed the study. ES, TN, TSH, SB and SV recruited the patients and gathered the clinical data. SV analyzed the data and drafted the manuscript. All authors contributed to the writing of the manuscript and approved the final version.

Declaration of Competing Interest

None.

References

1. Zimmermann P., Curtis N.. The effect of antibiotics on the composition of the intestinal microbiota - a systematic review. *J Infect* 2019;**79**:471–89. doi:10.1016/j.jinf.2019.10.008.
2. Hörman A., Korpela H., Sutinen J., Wedel H., Hänninen M.L. Meta-analysis in assessment of the prevalence and annual incidence of Giardia spp. and Cryptosporidium spp. infections in humans in the Nordic countries. *Int J Parasitol* 2004;**34**:1337–46. doi:10.1016/j.ijpara.2004.08.009.
3. Jahan N., Khatoon R., Ahmad S. A comparison of microscopy and enzyme linked immunosorbent assay for diagnosis of Giardia lamblia in human faecal specimens. *J Clin Diagn Res* 2014;**8** DC04-6. doi:10.7860/JCDR/2014/9484.5087.
4. Ordóñez-Mena J.M., McCarthy N.D., Fanshawe T.R. Comparative efficacy of drugs for treating giardiasis: a systematic update of the literature and network meta-analysis of randomized clinical trials. *J Antimicrob Chemother* 2018;**73**:596–606. doi:10.1093/jac/dkx430.
5. Panja S.K.. Treatment of trichomoniasis with metronidazole rectal suppositories. *Br J Vener Dis* 1982;**58**:257–8. doi:10.1136/sti.58.4.257.
6. McLean A., Ioannides-Demos L., Somogyi A., Tong N., Spicer J. Successful substitution of rectal metronidazole administration for intravenous use. *Lancet* 1983;**1**:41–3. doi:10.1016/s0140-6736(83)91573-8.
7. de Boer C.N., Thornton J.G. Prophylactic short course rectal metronidazole for cesarean section. A double-blind controlled trial of a simple low cost regimen. *Int J Gynaecol Obstet* 1989;**28**:103–7. doi:10.1016/0020-7292(89)90468-2.
8. Lau A.H., Lam N.P., Piscitelli S.C., Wilkes L., Danziger L.H. Clinical pharmacokinetics of metronidazole and other nitroimidazole anti-infectives. *Clin Pharmacokinet* 1992;**23**:328–64. doi:10.2165/00003088-199223050-00002.
9. Mattila J., Männistö P.T., Mäntylä R., Nykänen S., Lamminsivu U. Comparative pharmacokinetics of metronidazole and tinidazole as influenced by administration route. *Antimicrob Agents Chemother* 1983;**23**:721–5. doi:10.1128/aac.23.5.721.

Svetlana Vakkilainen*
Tea Nieminen
Susanna Björkbacka
Tarja Saavalainen-Hakala
Eeva Salo
New Children's Hospital, Pediatric Research Center, University of Helsinki and HUS Helsinki University Hospital, Stenbäckinkatu 9, PL 347, 00290 Helsinki, Finland
*Corresponding author.
E-mail address: svetlana.vakkilainen@hus.fi (S. Vakkilainen)

Accepted 29 August 2020
Available online 1 September 2020

https://doi.org/10.1016/j.jinf.2020.08.050

© 2020 The British Infection Association. Published by Elsevier Ltd. All rights reserved.

Cardiovascular disease as a risk factor of disease progression in COVID-19: The corrected effect size and forest plot

Dear Editor,

While the world is in lockdown for months since December of 2019 due to novel coronavirus disease (COVID-19) pandemic, a lot of research is in progress to find out various risk factors associated with COVID-19 progression and related mortalities.[1]

We read with great interest, the recent and very informative article by Zheng et al.,[2] who performed a meta-analysis to identify various risk factors such as; demographical (male, age, current smoking), comorbidities (diabetes, hypertension, malignancy, respiratory disease and cardiovascular disease), and other laboratory variables for the progression of COVID-19.

Firstly, we have a concern related to the result on the presence of cardiovascular disease (CVD) in association with COVID-19. The reported result for this pooled-outcome based on ten included studies has been shown to be statistically significant with a higher proportion of CVD in critical/mortal group compared to the non-critical group of COVID-19 patients. The pooled effect size for this association has been reported as odds ratio (OR) with its 95% confidence interval (CI) levels (OR=5.19, 95% CI=3.25–8.29, $P<0.00001$). However, upon proper examination of the reported forest plot and the included studies, we observed that the input data for one included study by Shi Y et al.,[3] was wrong and therefore the outcome 'effect size' for this study has been shown to be 'Not Estimable' (Fig. 3. of Zheng et al.).[2]

It is very much important for proper data inputs and thorough checks for its correctness by multiple authors while performing a meta-analysis. In the reported meta-analysis, the CVD events and total number under critical/mortal group from a study by Shi Y et al.,[3] have been recorded for meta-analysis as 49 and 4, respectively. It is for this reason, the effect-size has been found to be 'Not Estimable' in the respective forest plot (Fig. 3. of Zheng et al.).[2] We, upon a thorough review of the study by Shi Y et al., noticed that the actual values are 4 and 49 for CVD events and total number, respectively.[3]

Secondly, by further inspecting the forest plot, in addition to inappropriate data inputs, the study weights have been noticed to be very disproportionate to each other (minimum 1.7 & maximum 28.7).[2] It is a known myth to choose either fixed or random effects model for a meta-analysis based on the heterogeneity statistics, particularly fixed effects model is not a viable method when objective is to measure the effect size of group level variables.[4]

Therefore, in this letter we updated the forest plot and the effect-size characteristics for the relationship between CVD and COVID-19 progression (including the missing data for a study & random effects model which considers both within and between study variability). According to the random effects model used (Fig. 1), the study weights were found to better distributed than in the fixed effects model (minimum 3.1 & maximum 18.0), and the results showed a significantly higher proportion of CVD in critical/mortal group compared to the non-critical group of COVID-19 patients (OR=4.78, 95% CI=2.71–8.42, $P<0.00001$). Considering the limitation that the COVID-19 patients with underlying CVD may also have other comorbidities, the use of random effects model would provide a better statistic and the obtained result should be interpreted with a caution to the limitation of other overlapping comorbidities.

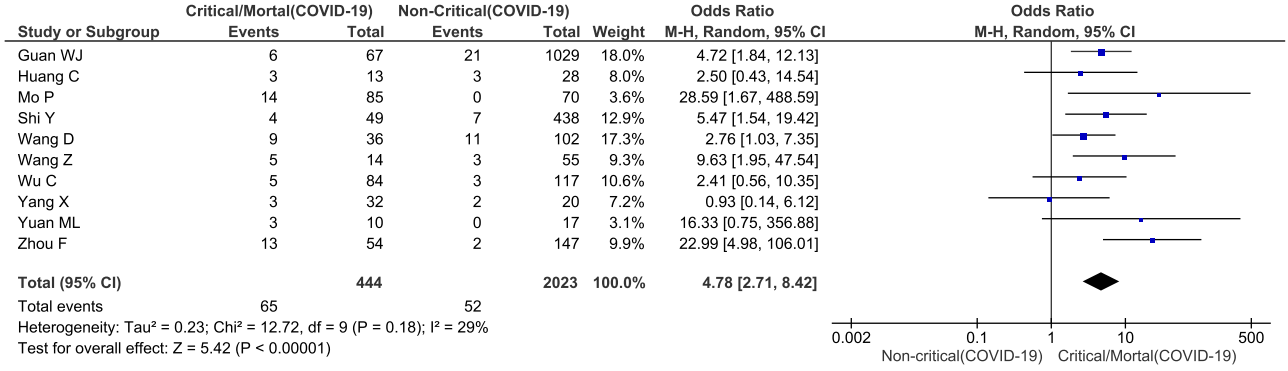

Fig. 1. Forest plot for cardiovascular disease comorbidity between critical/mortal and non-critical COVID-19 patients.

References

1. Chan J.F., Yuan S., Kok K.H., et al. A familial cluster of pneumonia associated with the 2019 novel coronavirus indicating person-to-person transmission: a study of a family cluster.[J]. *Lancet* 2020;**395**(10223):514–23 doi. doi:10.1016/s0140-6736(20)30154-9.
2. Zheng Z., Peng F., Xu B., et al. Risk factors of critical & mortal COVID-19 cases: a systematic literature review and meta-analysis [published online ahead of print, 2020 Apr 23]. *J Infect.* 2020 S0163-4453(20)30234-6doi. doi:10.1016/j.jinf.2020.04.021.
3. Shi Y., Yu X., Zhao H., et al. Host susceptibility to severe COVID-19 and establishment of a host risk score: findings of 487 cases outside Wuhan.[J]. *Crit Care* 2020;**24**(1):108 doi. doi:10.1186/s13054-020-2833-7.
4. Dieleman J.L., Templin T.. Random-effects, fixed-effects and the within-between specification for clustered data in observational health studies: a simulation study.[J]. *PLoS ONE* 2014;**9**(10):e110257 doi. doi:10.1371/journal.pone.0110257.

Seshadri Reddy Varikasuvu*
Department of Biochemistry, All India Institute of Medical Sciences (AIIMS), Deoghar, Jharkhand, India

Naveen Dutt
Department of Respiratory Medicine, All India Institute of Medical Sciences (AIIMS), Jodhpur, Rajasthan, India

*Corresponding author: Department of Biochemistry, All India Institute of Medical Sciences (AIIMS), Deoghar, Jharkhand 814152, India.
E-mail address: lifeschemistry@live.com (S.R. Varikasuvu)

Accepted 20 May 2020
Available online 27 May 2020

https://doi.org/10.1016/j.jinf.2020.05.038

© 2020 The British Infection Association. Published by Elsevier Ltd. All rights reserved.

Identification of a novel HIV-1 second-generation Circulating Recombinant Form CRF109_0107 in China

Dear Editor,

Inter-subtype recombinants play an increasingly central role in the complex and dynamic HIV/AIDS epidemic. At present, 106 Circulate recombinant forms (CRFs) have been identified worldwide. In 2000, CRF07_BC and CRF08_BC were first reported in China, and novel CRFs identified in China has soared since 2013. Inter-subtype recombinant viruses, especially CRF01_AE and CRF07_BC, have become the predominant strains of the HIV-1 epidemic in China.[1] The double infection between CRFs established more optimal conditions for the second-generation recombination,[2] and many second-generation recombinants were represented by the recombination of CRF01_AE and CRF07_BC fragments, such as CRF79_0107,[3] CRF80_0107,[4] and CRF102_0107[5]. In the present study, we identified a newly emerging second-generation HIV-1 CRF called CRF109_0107, consisting of CRF01_AE and CRF07_BC fragments. Through the evolution analysis of all CRF01_AE and CRF07_BC recombinant fragments, we uncovered the evolutionary history of CRF109_0107 finally.

Plasma samples were collected from two HIV-positive patients (LS11584 and LS14250) who were infected through sexual transmission in Shenzhen, China. The sequence BJSJS2016S195 is obtained from the Los Alamos HIV Sequence Database with the full-length *gag* (HXB2:790–2292 nt) and *pol* (HXB2:2085–5096 nt) gene sequences in the Shijingshan district of Beijing, China. There was no epidemiologic link among these three individuals. All participants gave a written, signed informed consent prior to plasma specimen collection and subsequent analyses. Basic epidemiological data are presented in Table 1.

Viral RNAs were extracted from plasma samples using the High Pure Viral RNA Kit (Roche, Germany). Then, the near full-length genome (NFLG) was amplified through reverse transcription (RT)-nested polymerase chain reaction utilizing Superscript™ IV First-strand Synthesis System (Invitrogen) and Platinum™ Taq DNA Polymerase High Fidelity (Invitrogen). After PCR positive products were purified and sequenced, all sequence fragments were edited and assembled into contiguous sequences using the ContigExpress project. Finally, the near full-length genome (NFLG) of the LS11584 (HXB2:786–9604 nt) and the LS14250 (HXB2:771–9613 nt) were obtained. These two NFLG sequences were submitted to the Basic Local Alignment Search Tool (BLAST) analysis, and the most closely related and highest similarity (>95%) partial sequence of BJSJS2016S195 *gag-pol* region (HXB2:790–5096 nt) was obtained. To demonstrate possible inter-subtype mosaicism, the jumping profile hidden Markov model (jpHMM) (http://jphmm.gobics.de/submission_hiv) was used to perform recombination breakpoint analysis with the default option on these three sequences. The three sequences were aligned with HIV reference sequences (https://www.hiv.lanl.gov) covering the major HIV-1 pure subtypes and CRFs using MAFFT v7.0. Neighbor-joining (NJ) method and the Kimura two-parameter model were used to build a phylogenetic tree by the MEGA 6.0 software. The time of the most recent common ancestor (tMRCA) of CRF109_0107 through the evolution analysis was uncovered by using BEAST v1.7.5.

Phylogenetic analysis revealed that these three sequences formed a distinct monophyletic branch with a high bootstrap value of 100%, distantly related to all known HIV-1 subtypes/CRFs (Fig. 1A). The recombination analysis showed that the two NFLG sequences were composed of CRF01_AE and subtypes B and C (Fig. 1B). And the *gag-pol* region sequence of BJSJS2016S195 has the same breakpoints as the corresponding regions of LS11584 and LS14250. Subtype B and Subtype C fragments of CRF109_0107 were further phylogenetic analysis and submitted to BLAST, the results showed the highest similarity to (>95%) CRF07_BC (Fig. 1C).

A total of 13 recombinant breakpoints were found at HXB2 positions according to the recombination analysis as follows: I(790–1169 nt) CRF01_AE, II(1170–1840 nt) Subtype B, III(1841–2166 nt) CRF01_AE, IV(2167–2466 nt) Subtype B, V(2467–3038 nt) CRF01_AE, VI(3039–3295 nt) Subtype B, VII(3296–4238 nt) CRF01_AE, VIII(4239–4613 nt) Subtype C, IX(4614–5157 nt) CRF01_AE, X(5158–5886 nt) Subtype C, XI(5887–6383 nt) CRF01_AE, XII(6384–8442 nt) Subtype C, XIII(8443–9411 nt) CRF01_AE, using HXB2 as a reference (Fig. 1C). Subregion phylogenetic analyses of 13 genomic segments were further conducted to explore their likely parental lineages. The high bootstrap values in the phylogenetic tree supported a close relationship with CRF01_AE or CRF07_BC subtype references respectively. Subregion phylogenetic analyses indicated that the segment I, III, V, VII, IX, XI, and XIII of CRF109_0107 belonged to the CRF01_AE cluster 5,[6] which is mainly circulating among high-risk sexual behaviors in MSM and Heterosexual population in China (Fig. 2A). The segment II, IV, VI, VIII, X, and XII of CRF109_0107 were clustered with the CRF07_BC cluster, which is also identified among high-risk sexual behaviors in the MSM population[7,8] (Fig. 2B). The segments of CRF109_0107 are closely related to the clusters associated with the sexually transmitted population according to the sub-regional analysis, suggesting that CRF109_0107 may be predominantly prevalent in the MSM and Heterosexual population.

The Bayesian analysis shows that the (tMRCA) of the CRF01_AE regions(segments I+III+V+VII+IX and segments XI+XIII) from

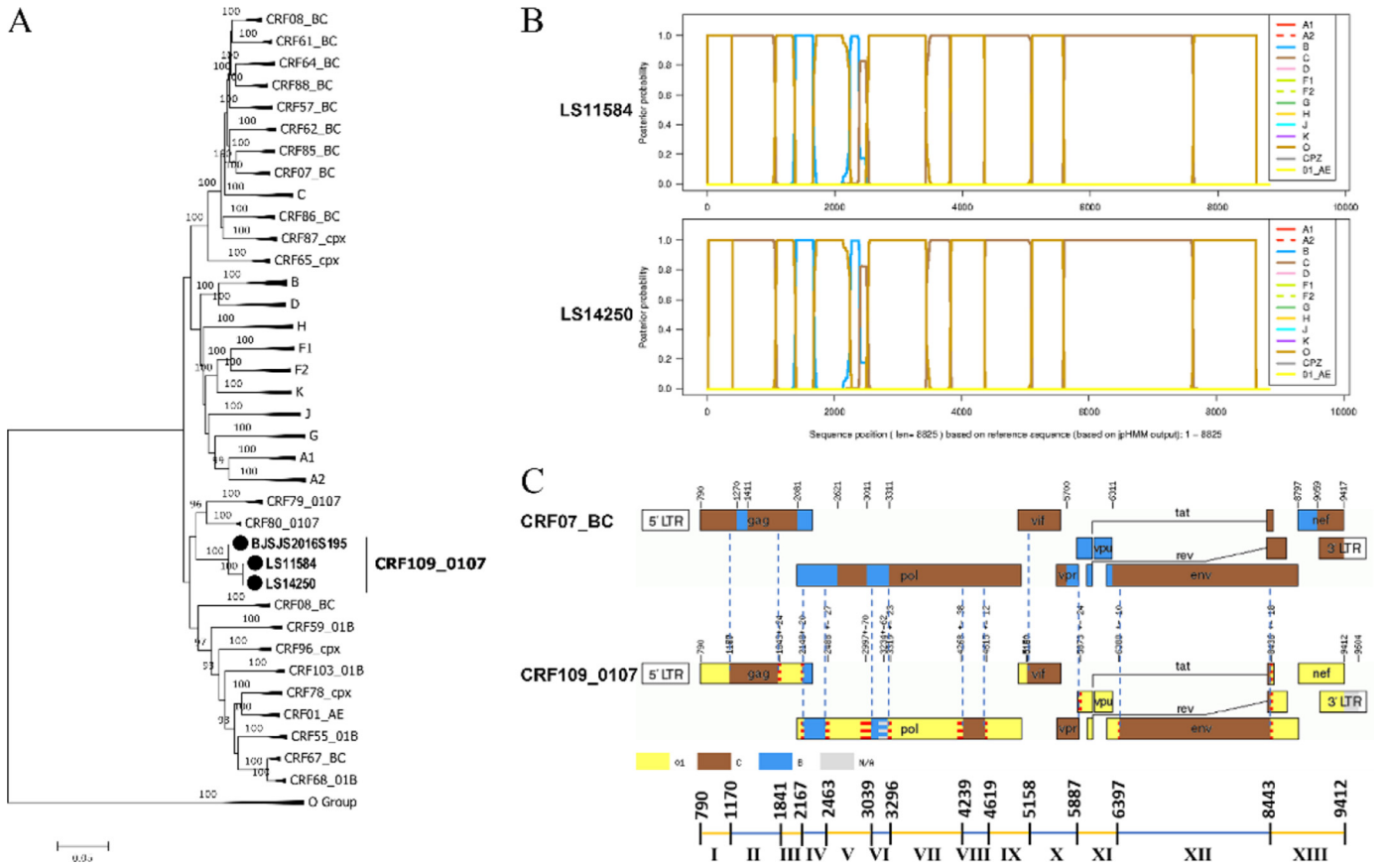

Fig. 1. Phylogenetic and recombinant analyses based on near full-length HIV-1 genome sequences in CRF109_0107. **(A)**Two NFLG sequences (LS11584 and LS14250) together with the *gag-pol* region sequences (HXB2:790-5096nt) of BJSJS2016S195 in this study were further aligned with HIV reference sequences (https://www.hiv.lanl.gov) covering the major HIV-1 pure subtypes and CRFs using Clustal W in the BioEdit 7.2.5 program. Neighbor-joining (NJ) method and the Kimura two-parameter model were used to build a phylogenetic tree by using the MEGA 6.0 software. The sequences of CRF109_0107 were marked with "•". **(B)** Posterior probabilities of the subtypes. **(C)** Comparison of genomic maps between CRF07_BC and CRF109_0107. All these maps were generated using jumping profile hidden Markov model (jpHMM). CRF109_0107 strains are highlighted in yellow (CRF01_AE region) and blue (CRF07_BC region).

CRF109_0107 were predicted in 2012.4, [95% highest probability density (HPD): 2010.3, 2018.3] and 2013.8, [95% highest probability density (HPD): 2013.8, 2014.4], respectively (Fig. 2C). The (tMRCA) of the CRF07_BC regions (segments II+IV+VI+VIII and segments X+XII) from CRF109_0107 were predicted in 2012.4, [95% highest probability density (HPD): 2010.4, 2018.4] and 2013.8, [95% highest probability density (HPD): 2013.8, 2014.5], respectively (Fig. 2D). The recombinant fragments (segments I-IX and segments X-XIII) originated around 2012.4 and 2013.8, respectively. Hence, it is inferred that the CRF109_0107 formed a recombination in two time periods, respectively.

HIV-1 novel CRFs have been increased rapidly in individuals with high-risk sexual behaviors. CRF55_01B has been confirmed to be an epidemic in the MSM population in Shenzhen.[9] CRF65_cpx, which originated in Yunnan,[10] was also found to have spread to other parts of China after entering the MSM population.[11] Frequent high-risk sexual behavior led to the rapidly spread and to a higher genetic diversity of HIV, which may have caused the incidence of a high level of recombination.[12] Second-generation recombinant virus, CRF79_0107, caused by double infection has also spread rapidly to 5 provinces in individuals with high-risk sexual behaviors in China. It is especially worth noting that, with the rapid spread of CRF01_AE and CRF07_BC among MSM, more and more new second-generation CRFs represented by the recombination of CRF01_AE and CRF07_BC will be identified and found spreading in high-risk populations in the future.

In summary, a novel HIV-1 circulating recombinant form CRF109_0107 whose genome consists of CRF01_AE and CRF07_BC

Table 1
Demographic characteristics of study subjects infected with CRF109_0107.

Strain name	Sampling year	Sampling region	Gender	Age	Ethnic group	Marriage	Risk factor	Accession no.
LS11584	2014	Shenzhen, Guangdong	Male	45	Han	unmarried	MSM	MT919517
LS14250	2014	Shenzhen, Guangdong	Male	40	Han	married	HETE	MT919518
BJSJS2016S195	2016	Beijing	Male	33	unknown	unknown	unknown	MH921062.MH921177

*MH921062: BJSJS2016S195 Gag Region; MH921177: BJSJS2016S195 Pol Region.

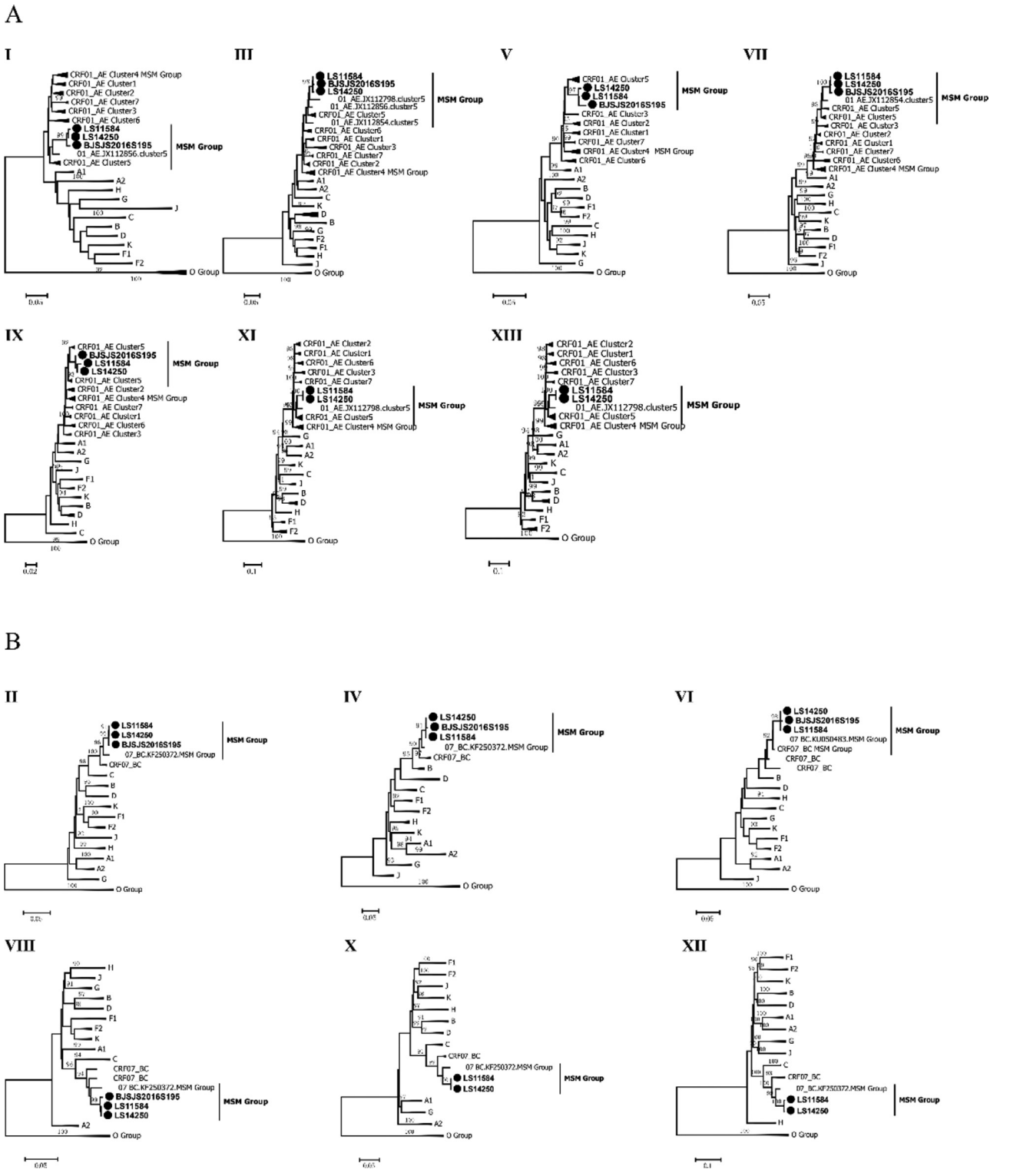

Fig. 2. Subregion tree analyses and maximum clade credibility (MCC) trees of CRF109_0107. (A) Segments I, III, V, VII, IX, XI and XIII (HXB2: 790-1169nt, 1841-2166nt, 2467-3038nt, 3296-4238nt, 4614-5157nt, 5887-6383nt and 8443-9411nt) from CRF109_0107 genome map is the representative of all CRF01_AE segments inserted into the mosaic structure. (B) Segments II, IV, VI, VIII, Xand XII(1170-1840nt, 2167-2466nt, 3039-3295nt, 4239-4613nt, 5158-5886nt and 6384-8442nt) from CRF109_0107 genome map is the representative of all CRF07_BC segments inserted into the mosaic structure. The subregion neighbor-joining tree was constructed based on Kimura 2-parameter model of nucleotide substitution with 1000 bootstrap replicates, and gamma distributed rates among sites were applied in MEGA6 software. The sequences of CRF109_0107 were marked with "•". Only bootstrap values >90% are presented at the corresponding nodes of the tree. (C) MCC trees display recombinant fragments CRF01_AE regions (segments I+III+V+VII+IXand segments XI+XIII). (D) MCC trees display recombinant fragments CRF07_BC regions (segments II+IV+VI+VIIIand segments X+XII). Timescale is shown at the bottom of the tree. The mean tMRCA and 95% highest probability density (HPD) for the key nodes are displayed. CRF109_0107 strains are highlighted in yellow (CRF01_AE region) and blue (CRF07_BC region). (For interpretation of the references to colour in this figure legend, the reader is referred to the web version of this article.)

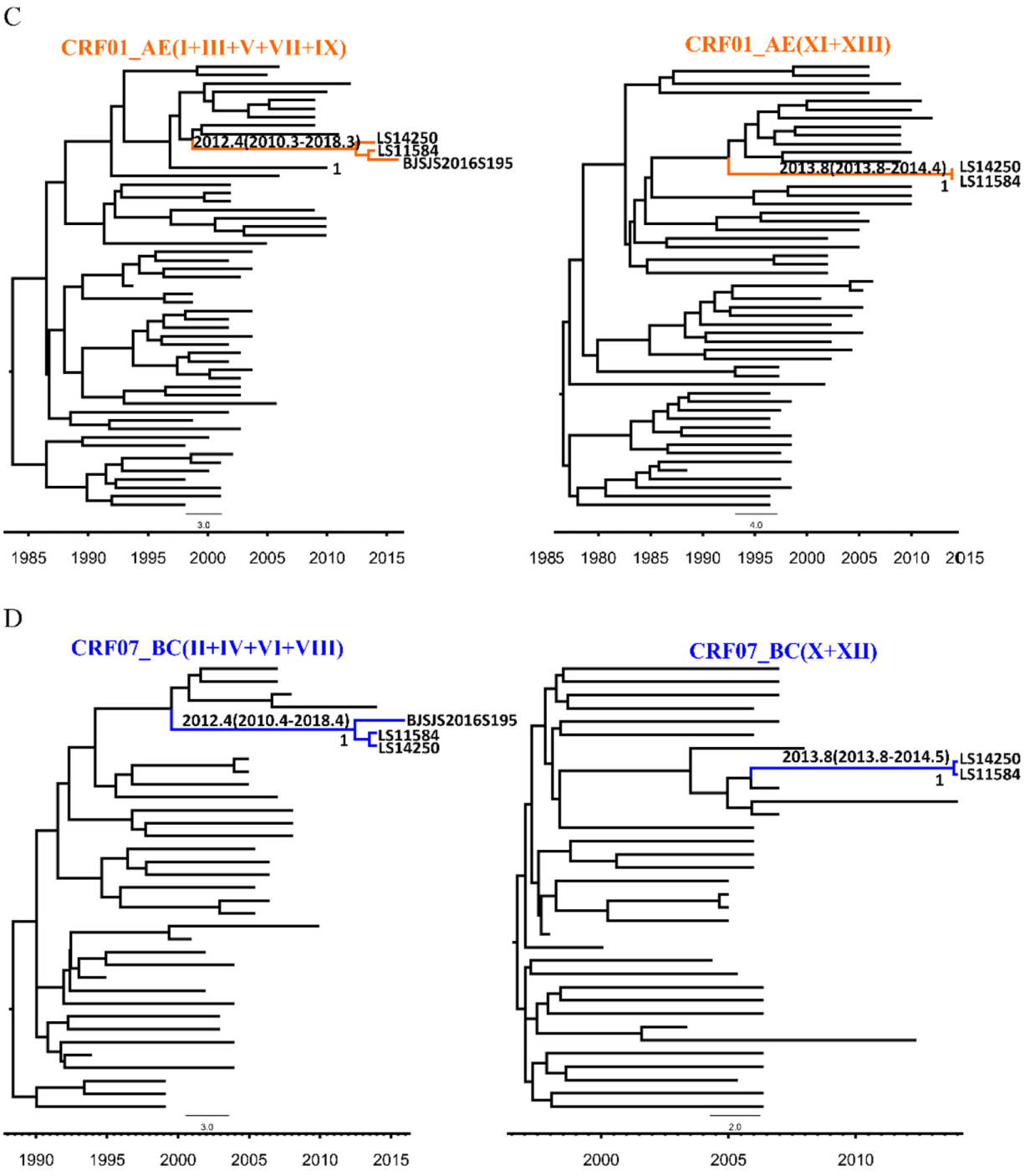

Fig. 2. Continued

with 12 breakpoints and 13 segments was defined, which has a more complex recombinant form than others. The emergence of CRF109_0107 indicates that CRF01_AE and CRF07_BC have been spreading in the same population. The complex social behaviors of MSM and Heterosexual population will further complicate the epidemic of HIV-1 in China. More and more second-generation CRFs comprised of CRF01_AE and CRF07_BC in the future will emerge. Therefore, surveillance will be necessary in specific high-risk populations in China.

Declaration of Competing Interests

No competing financial interests exist.

Funding

This study was supported by the NSFC (81773493, 31800149, 31900157), the State Key Laboratory of Pathogen and Biosecurity (AMMS), the National 13th Five-Year Grand Program on Key Infectious Disease Control (2018ZX10721102, 2018ZX10732101–001–003).

Sequences Data

The gene sequences of LS11584 and LS14250 were deposited in the GenBank with the accession number: MT919517 and MT919518, respectively. The gene sequences of BJSJS2016S95

were deposited in the GenBank with the accession number: MH921062 *gag* region (HXB2:790–2,292 nt), MH921177 *pol* region (HXB2:2,085–5,096 nt), respectively.

Acknowledgments

The authors thank all of the participants and peer workers.

References

1. Li X., Li W., Zhong P., et al. Nationwide trends in molecular epidemiology of HIV-1 in China. *AIDS Res Hum Retroviruses* 2016;**32**(9):851–9 09.
2. Luan H., Han X., Yu X., et al. Dual infection contributes to rapid disease progression in men who have sex with men in China. *J Acquir Immune Defic Syndr* 2017;**75**(4):480–7 08 01.
3. Li Y., Feng Y., Li F., et al. Genome sequence of a Novel HIV-1 circulating recombinant form (CRF79_0107) identified from Shanxi, China. *AIDS Res Hum Retroviruses* 2017;**33**(10):1056–60.
4. Zhang Y., Pei Z., Li H., et al. Characterization of a Novel HIV-1 Circulating Recombinant Form (CRF80_0107) Among Men Who Have Sex with Men in China. *AIDS Res Hum Retroviruses* Apr 2019;**35**(4):419–23.
5. Li X., Wu J., Zhang Y., et al. Characterization Of A Novel HIV-1 S-generation circulating recombinant form(CRF102_0107) among men who have sex with men in Anhui, China. *J Infect* 2019;**79**(6):612–25.
6. Feng Y., He X., Hsi J.H., et al. The rapidly expanding CRF01_AE epidemic in China is driven by multiple lineages of HIV-1 viruses introduced in the 1990s. *AIDS* 2013;**27**(11):1793–802.
7. Feng Y., Takebe Y., Wei H., et al. Geographic origin and evolutionary history of China's two predominant HIV-1 circulating recombinant forms, CRF07_BC and CRF08_BC. *Sci Rep* 2016;**6**:19279.
8. Wang X., Wu Y., Mao L., et al. Targeting HIV prevention based on molecular epidemiology among deeply sampled subnetworks of men who have sex with men. *Clin Infect Dis* 2015;**61**(9):1462–8.
9. Zhao J., Cai W., Zheng C., et al. Origin and outbreak of HIV-1 CRF55_01B among MSM in Shenzhen, China. *J Acquir Immune Defic Syndr* 2014;**66**(3):e65–7 Jul 01.
10. Feng Y., Wei H., Hsi J., et al. Identification of a novel HIV Type 1 circulating recombinant form (CRF65_cpx) composed of CRF01_AE and subtypes B and C in Western Yunnan, China. *AIDS Res Hum Retroviruses* 2014;**30**(6):598–602.
11. Liu Y., Gui T., Jia L., et al. Phylogenetic analysis of HIV-1 CRF65_CPX Reveals Yunnan Province is still a source contributing to the spread of HIV-1 in China. *J Acquir Immune Defic Syndr* 2015;**70**(3):e120–2 Nov 01.
12. Trujillo L., Chapin-Bardales J., German E.J., Kanny D., Wejnert C. Trends in sexual risk behaviors among hispanic/latino men who have sex with men - 19 Urban Areas, 2011-2017. *MMWR Morb Mortal Wkly Rep* 2019;**68**(40):873–9 Oct 11.

Xiaorui Wang[1]
Department of Microbiological Laboratory Technology, School of Public Health, Cheeloo College of Medicine, Shandong University, Key laboratory for the prevention and control of infectious diseases (key laboratory of China's "13th Five-Year", Shandong University), 44 Wenhua, West Street, Lixia District, Jinan 250012, Shandong Province, China
Department of AIDS Research, State Key Laboratory of Pathogen and Biosecurity, Beijing Institute of Microbiology and Epidemiology, 20 Dongda Street, Fengtai District, Beijing 100071, China

Jin Zhao[1]
Shenzhen Center for Disease Control and Prevention, Shenzhen, 518055, Guangdong, China

Xi Li, Hanping Li, Yu Zhang, Yongjian Liu
Department of AIDS Research, State Key Laboratory of Pathogen and Biosecurity, Beijing Institute of Microbiology and Epidemiology, 20 Dongda Street, Fengtai District, Beijing 100071, China

Lin Chen, Chenli Zheng
Shenzhen Center for Disease Control and Prevention, Shenzhen, 518055, Guangdong, China

Lei Jia, Jingwan Han, Tianyi Li, Xiaolin Wang, Jingyun Li
Department of AIDS Research, State Key Laboratory of Pathogen and Biosecurity, Beijing Institute of Microbiology and Epidemiology, 20 Dongda Street, Fengtai District, Beijing 100071, China

Hongling Wen*
Department of Microbiological Laboratory Technology, School of Public Health, Cheeloo College of Medicine, Shandong University, Key laboratory for the prevention and control of infectious diseases (key laboratory of China's "13th Five-Year", Shandong University), 44 Wenhua, West Street, Lixia District, Jinan 250012, Shandong Province, China

Lin Li*
Department of AIDS Research, State Key Laboratory of Pathogen and Biosecurity, Beijing Institute of Microbiology and Epidemiology, 20 Dongda Street, Fengtai District, Beijing 100071, China

*Corresponding authors.
E-mail addresses: wenhongling@sdu.edu.cn (H. Wen), dearwood@sina.com (L. Li)

[1] Xiaorui Wang and Jin Zhao contributed equally to this work.

Identification of CRF109_0107 in China
Accepted 14 September 2020
Available online 16 September 2020

https://doi.org/10.1016/j.jinf.2020.09.007

Crown Copyright © 2020 The Authors. Published by Elsevier Ltd on behalf of The British Infection Association. This is an open access article under the CC BY-NC-ND license (http://creativecommons.org/licenses/by-nc-nd/4.0/).